

(A New Proposal to Jefferson Laboratory PAC 32)

**Precision Measurement of the Parity-Violating Asymmetry in Deep Inelastic
Scattering off Deuterium using Baseline 12 GeV Equipment in Hall C**

D.S. Armstrong, T. Averett, J.M. Finn, K. Grimm, and C. Perdrisat

College of William and Mary, Williamsburg, VA 23187, USA

J. Arrington, D. Geesaman, K. Hafidi, R. Holt,

P.E. Reimer (Co-Spokesperson) *, and P. Solvignon

Physics Division, Argonne National Laboratory, Argonne, IL 60439, USA

E. Beise and H. Breuer

University of Maryland, College Park, MD 20742, USA

W. Bertozzi, S. Gilad, J. Huang, B. Moffit,

P. Monaghan, N. Muangma, A. Puckett, and X.-H. Zhan

Massachusetts Institute of Technology, Cambridge, MA 02139, USA

P. Bosted, A. Camsonne, J.-P. Chen, E. Chudakov, A. Deur,

J.-O. Hansen, D.W. Higinbotham, R. Michaels, and A. Saha

Thomas Jefferson National Accelerator Facility, Newport News, VA 23606, USA

G.D. Cates, N. Liyanage, B.E. Norum,

K. Paschke (Co-Spokesperson) †, and X.-C. Zheng (Co-Spokesperson) ‡

University of Virginia, Charlottesville, VA 22904, USA

R. Holmes

Syracuse University, Syracuse, NY 13244, USA

T. Holmstrom

Randolph-Macon College, Ashland, VA 23005, USA

* email: reimer@anl.gov

† email: paschke@jlab.org

‡ email: xiaochao@jlab.org

K. Johnston, N. Simicevic, and S.P. Wells

Louisiana Tech University, Ruston, LA 71272, USA

P.M. King and J. Roche

Ohio University, Athens, OH 45701, USA

S. Kowalski

Massachusetts Institute of Technology, Cambridge, MA 02139, USA

K. Kumar and D. McNulty

University of Massachusetts, Amherst, MA 01003, USA

A. Lukhanin, Z.-E. Meziani, and B. Sawatzky

Temple University, Philadelphia, PA 19122, USA

P. Markowitz

Florida International University, Miami, FL 33199, USA

P.A. Souder

Syracuse University, Syracuse, New York 13244, USA

(Dated: June 20, 2007)

We propose a measurement of the parity-violating (PV) asymmetry in $\vec{e}^{-2}\text{H}$ deep inelastic scattering (DIS) at $Q^2 = 3.3 \text{ GeV}^2$, $\langle W^2 \rangle = 7.3 \text{ GeV}^2$ and $\langle x \rangle = 0.34$. The experiment will use the baseline 12 GeV Hall C spectrometer with a 40 cm liquid deuterium target and an 85 μA beam with 80% polarization. The predicted asymmetry is approximately 280 ppm at these kinematics, which is relatively large for a PV asymmetry. A relative statistical error of 0.5% is achievable with 28 days of production beam. An additional 8 days would be required for various systematic studies. The goal for the systematic uncertainty would be to limit its effect to the size of the statistical error. While the errors from corrections to the asymmetry from beam effects and backgrounds should be straightforward to control, normalization

errors especially from the beam polarization at this level of accuracy will present a significant, although not insurmountable, challenge.

If hadronic effects are under control, these data can be used to obtain, with unprecedented precision, a linear combination of two poorly known low energy weak neutral current coupling constants: $2C_{2u} - C_{2d}$. Within the context of the Standard Model, these coupling constants are functions of a single parameter, the weak mixing angle $\sin^2 \theta_W$. At the proposed precision, the measurement would provide unique constraints on physics beyond the Standard Model at the multi-TeV scale. Interpreting the asymmetry measurement at the proposed level of accuracy in terms of Standard Model parameters will require tight constraints on several aspects of nucleon structure at high Bjorken x that are beyond the scope of this single measurement. These issues, interesting in their own right, are discussed briefly. It is likely that the proposed measurement will be part of a larger program that would use PV-DIS to search for physics beyond the Standard Model as well as to address long-standing fundamental issues in valence quark physics.

Contents

1. Introduction	1
1.1. The Running of $\sin^2 \theta_W$	1
1.2. Phenomenological WNC Couplings at Low Q^2	2
2. Parity Violation in Deep Inelastic Scattering and the Standard Model	4
2.1. Parity Violation in Deep Inelastic Scattering	5
2.2. Exploring New Physics Beyond the Standard Model	8
2.2.1. Z' Searches	9
2.2.2. Compositeness and Leptoquarks	9
2.2.3. Supersymmetry (SUSY)	11
3. Experimental Configuration and Systematic Uncertainties	13
3.1. The Measurement with the 12 GeV Baseline Spectrometers	13
3.2. Particle Identification and Pion Contamination	14
3.3. Pair Production Background	18
3.4. Rescatter Background	19
3.5. Polarized Electron Source	21
3.6. Beam Line and Polarimetry	22
3.7. Liquid Deuterium Target	24
3.8. Data Acquisition	27
3.9. Determination of Q^2	29
3.10. Radiative Corrections	30
3.11. Summary of Experimental Systematic Uncertainties	32
4. Hadronic Physics Issues	32
4.1. Uncertainty from Parton Distributions	33
4.2. Uncertainty in R_{LT}	33
4.3. Higher-Twist Effects	33
4.4. Charge Symmetry Violation (CSV)	35
4.5. Hadronic Uncertainty Summary	39

5. Beam Time Request	40
6. Complementarity with Possible Large Acceptance Device Program	41
7. Conclusion	42
A. Relation to PV-DIS at 6 GeV (JLab E05-007)	43
B. Technical Participation of Argonne National Laboratory	44
C. Contributions from the University of Virginia	44
References	44

1. INTRODUCTION

The Standard Model of particle physics describes three of the four known fundamental interactions of nature. To date, almost all experimental tests of the three forces described by the Standard Model have agreed with its predictions. However, the Standard Model falls short of being a complete theory of fundamental interactions, primarily because of its lack of inclusion of gravity, the fourth known fundamental interaction. In the electroweak sector, although there exist a large amount of data confirming the Standard Model at the level of a few parts per thousand, there also exist strong conceptual reasons (*e.g.*, the so-called high-energy desert from the weak scale $M_{\text{weak}} \approx 250$ GeV up to the Planck scale $M_P \approx 2.4 \times 10^{18}$ GeV) to believe that the Standard Model is only a piece of some larger framework [1]. This framework should provide answers to the conceptual puzzles of the Standard Model; but must also leave the $SU(3)_C \times SU(2)_L \times U(1)_Y$ symmetry of the Standard Model intact at $M_{\text{weak}} \approx 250$ GeV. Hence, there exists intense interest in the search for physics beyond the Standard Model.

1.1. The Running of $\sin^2 \theta_W$

The weak mixing angle, θ_W , is one of the fundamental parameters of the Standard Model. The tangent of the weak mixing angle represents the relative coupling strength of the $SU(2)_L$ and $U(1)_Y$ groups (g and g'). At the Z -pole, $Q^2 = M_Z^2$, the value of $\sin^2 \theta_W$ is experimentally well established to remarkable precision, $\sin^2 \theta_W[M_Z]_{\overline{MS}} = 0.23120 \pm 0.00015$ [2]; however, careful comparison of measurements involving purely leptonic and semi-leptonic electroweak currents shows a three standard deviation inconsistency. This strongly suggests additional physics not included in the Standard Model or that one or more of the experiments has significantly understated its uncertainties [3, 4].

One of the features of the Standard Model is that the value of $\sin^2 \theta_W$ will vary, or run, as a function of the momentum transfer, Q^2 , at which it is probed, so that the measurements at the Z -pole do not provide the complete picture. For $Q^2 < M_Z^2$, there are only three precise measurements. Atomic parity violation (APV) in Cs atoms [5] yields a result which while in agreement with Standard Model predictions has somewhat large uncertainties, and a difficult theoretical calculation is necessary to extract $\sin^2 \theta_W$ from the measured asym-

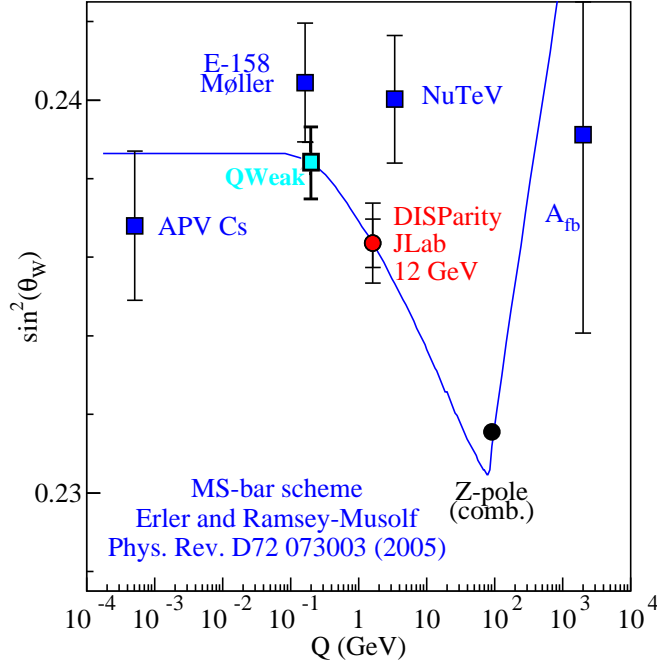


FIG. 1: The curve illustrates the running of $\sin^2 \theta_W$ [9] and the anticipated precision of the measurement described herein, as well as the measurements from APV [5], Fermilab NuTeV [6], SLAC E-158 Møller [7] and expected uncertainty of JLab QWeak [8].

metry. The NuTeV experiment at Fermilab measured $\sin^2 \theta_W$ through a careful comparison of neutrino and anti-neutrino deep inelastic scattering (DIS). Their result is approximately three standard deviations from Standard Model predictions [6]; although, the NuTeV result is not without considerable controversy. Most recently, the SLAC E-158 [7] experiment used the asymmetry in Moller scattering to determine a precise value of $\sin^2 \theta_W$ that is consistent with the Standard Model prediction. A fourth measurement, QWeak, is planned for Jefferson Laboratory [8], and will determine $\sin^2 \theta_W$ to 0.3% by measuring the weak charge of the proton. The results or projected data from these experiments are shown in Fig. 1 [9].

1.2. Phenomenological WNC Couplings at Low Q^2

Low energy precision tests of the electroweak Standard Model have and will continue to provide sensitive probes of possible extensions to the Standard Model. While all of the low energy measurements shown in Fig. 1 measure $\sin^2 \theta_W$, they do so in different ways and

thus have sensitivity to different possible extensions of the Standard Model. In lepton-quark scattering with two active flavors of quarks, there are six couplings. Assuming the Standard Model is complete, these are

$$C_{1u} = g_A^e g_V^u = -\frac{1}{2} + \frac{4}{3} \sin^2(\theta_W) \approx -0.19, \quad (1)$$

$$C_{1d} = g_A^e g_V^d = \frac{1}{2} - \frac{2}{3} \sin^2(\theta_W) \approx 0.35, \quad (2)$$

$$C_{2u} = g_V^e g_A^u = -\frac{1}{2} + 2 \sin^2(\theta_W) \approx -0.04, \quad (3)$$

$$C_{2d} = g_V^e g_A^d = \frac{1}{2} - 2 \sin^2(\theta_W) \approx 0.04, \quad (4)$$

$$C_{3u} = g_A^e g_A^u = -\frac{1}{2}, \text{ and} \quad (5)$$

$$C_{3d} = g_A^e g_A^d = \frac{1}{2}, \quad (6)$$

taking $\sin^2 \theta_W \approx 0.23$. Here, $g_{A(V)}^e$ is the electron's axial (vector) coupling and $g_{A(V)}^q$ is the axial (vector) coupling of a quark of flavor $q \in \{u, d\}$. Explicitly, the PV electron quark interaction can be written as

$$\mathcal{L}_{PV}^{eq} = \frac{G_\mu}{\sqrt{2}} \sum_q [C_{1q} \bar{e} \gamma^\mu \gamma_5 e \bar{q} \gamma_\mu q + C_{2q} \bar{e} \gamma^\mu e \bar{q} \gamma_\mu \gamma_5 q] . \quad (7)$$

Among the previously mentioned experiments, SLAC E-158 Møller is purely leptonic and not sensitive to these couplings. APV and QWeak are semileptonic but only access the Z -electron axial times Z -quark vector couplings, C_{1q} . Parity violating deep inelastic scattering (PVDIS) has a unique sensitivity to the C_{2q} couplings and the physics which they can uncover.

Table I summarizes the current knowledge of C_{iq} [10]. In contrast to C_{1q} , the weak coupling C_{2q} and C_{3q} are poorly known. From existing data, $2C_{2u} - C_{2d} = -0.08 \pm 0.24$. This constraint is poor and must be improved in order to enhance sensitivity to many possible extensions of the SM, such as quark compositeness and new gauge bosons. $e^{-2}\text{H}$ PVDIS can provide precise data on $2C_{2u} - C_{2d}$ which are not accessible through other processes. We expect to improve the uncertainty on $2C_{2u} - C_{2d}$ by a factor of 17. It will also impact our knowledge of the C_{3q} , since the only observable sensitive to the C_{3q} is the the CERN $\mu^\pm\text{C}$ DIS experiment [12], which provide a combination of C_{2q} and C_{3q} (see Table I).

Here, we propose to use PVDIS on a deuterium target to measure $\sin^2 \theta_W$ and more generally $2C_{2u} - C_{2d}$ as a test of the Standard Model. The experiment presented will use the

TABLE I: Existing data on P or C violating coefficients C_{iq} from Ref. [10]. The uncertainties are combined (in quadrature) statistical, systematic and theoretical uncertainties. The Bates e^-D quasi-elastic (QE) results on $C_{2u} - C_{2d}$ are from Ref. [11]. For some of the quantities listed here, global analysis gives slightly different values, please see Ref. [2] for the most recent updates.

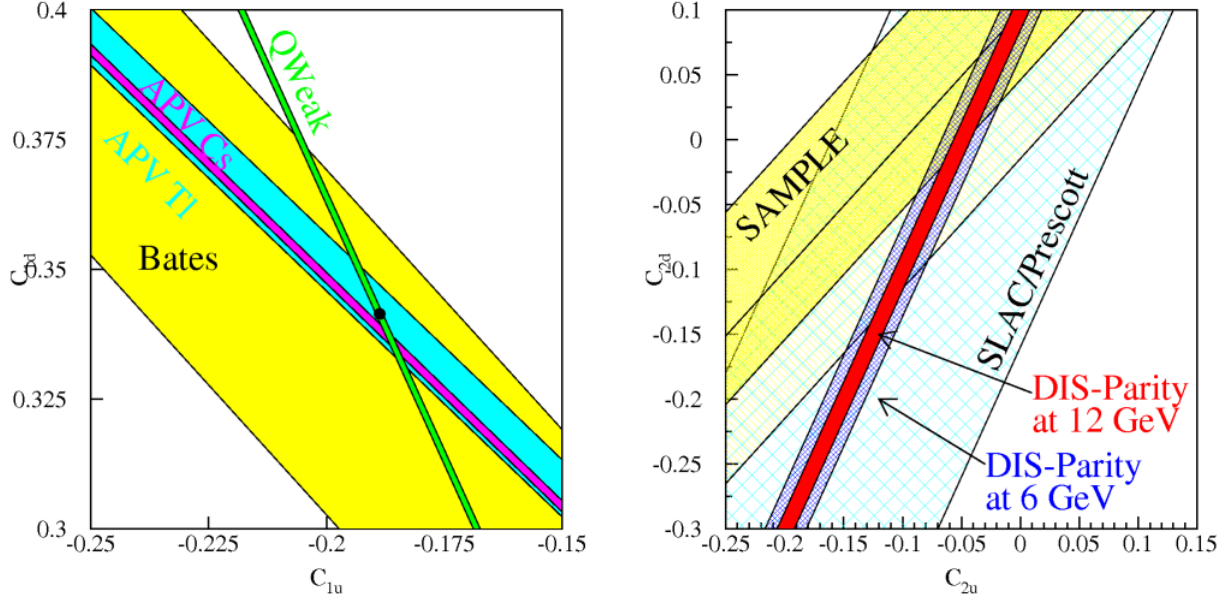
facility	process	$\langle Q^2 \rangle$ (GeV/c) ²	C_{iq} combination	result	SM value
SLAC	e^-D DIS	1.39	$2C_{1u} - C_{1d}$	-0.90 ± 0.17	-0.7185
SLAC	e^-D DIS	1.39	$2C_{2u} - C_{2d}$	$+0.62 \pm 0.81$	-0.0983
CERN	$\mu^\pm C$ DIS	34	$0.66(2C_{2u} - C_{2d})$ $+ 2C_{3u} - C_{3d}$	$+1.80 \pm 0.83$	+1.4351
CERN	$\mu^\pm C$ DIS	66	$0.81(2C_{2u} - C_{2d})$ $+ 2C_{3u} - C_{3d}$	$+1.53 \pm 0.45$	+1.4204
Mainz	e^-Be QE	0.20	$2.68C_{1u} - 0.64C_{1d}$ $+ 2.16C_{2u} - 2.00C_{2d}$	-0.94 ± 0.21	-0.8544
Bates	e^-C elastic	0.0225	$C_{1u} + C_{1d}$	0.138 ± 0.034	+0.1528
Bates	e^-D QE	0.1	$C_{2u} - C_{2d}$	-0.042 ± 0.057	-0.0624
Bates	e^-D QE	0.04	$C_{2u} - C_{2d}$	-0.12 ± 0.074	-0.0624
JLAB	e^-p elastic	0.03	$2C_{1u} + C_{1d}$	approved	+0.0357
--	¹³³ Cs APV	0	$-376C_{1u} - 422C_{1d}$	-72.69 ± 0.48	-73.16
--	²⁰⁵ Tl APV	0	$-572C_{1u} - 658C_{1d}$	-116.6 ± 3.7	-116.8

12 GeV upgrade baseline spectrometers in Jefferson Laboratory Hall C, namely the HMS and the SHMS. As will be shown in Sec. 2.1, the asymmetry due to parity violation is relatively large, providing statistical sensitivity in a modest beam time. This experiment builds on the approved 6 GeV PVDIS (E05-007) experiment [13], and shares much of its theoretical motivation.

2. PARITY VIOLATION IN DEEP INELASTIC SCATTERING AND THE STANDARD MODEL

Historically, parity violation in deep inelastic scattering (PVDIS) was one of the first tests of the Standard Model and an early measurement of PVDIS by Prescott *et al.* (SLAC

FIG. 2: The effective couplings C_{1u} , C_{1d} (left), C_{2u} and C_{2d} (right). The future Qweak experiment (purple band), combined with the APV-Cs result (red band), will provide the most precise data and the best Standard Model test on C_{1u} and C_{1d} . The SAMPLE result for $C_{2u} - C_{2d}$ at $Q^2 = 0.1$ (GeV/c)² and the projected results from the 6 GeV PVDIS experiment (E05-007, Phase I+II) [13] are shown. Assuming the SM prediction of $2C_{1u} - C_{1d}$, the value of $2C_{2u} - C_{2d}$ can be determined from the proposed measurement to $\Delta(2C_{2u} - C_{2d}) = 0.015$ (red band).



E122) in the 1970's served to establish the value of $\sin^2 \theta_W$ [14, 15] at $\sin^2 \theta_W \approx 1/4$. Since this groundbreaking experiment, parity violation has become an important tool not only for probing the Standard Model [5, 7, 8] but also for probing the structure of the nucleon [16, 17, 18].

2.1. Parity Violation in Deep Inelastic Scattering

Prior to the SLAC E122 experiment, electron beams were used solely as an electromagnetic probe of the nucleon because of the comparatively small amplitude of the weak neutral-current scattering at low energy. A number of facilities (JLab, SLAC, MIT-Bates, Mainz) have developed the capabilities to provide high enough luminosity to make studies of the weak neutral current and its couplings feasible. The weak neutral current can be accessed

by measuring a parity-violating asymmetry that is proportional to the interference term between weak and electromagnetic scattering amplitudes [19].

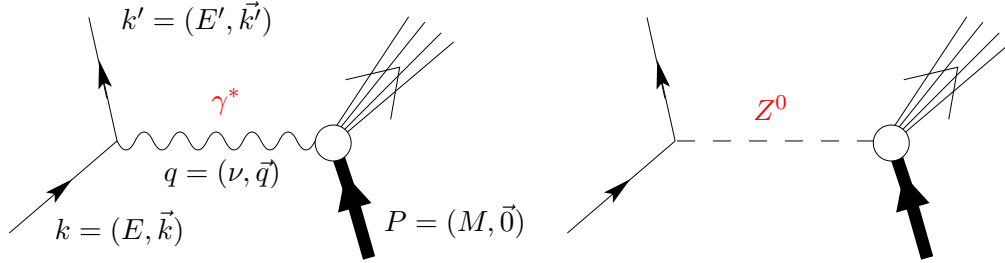


FIG. 3: Tree-level Feynman diagrams for electron scattering. The electron interacts with the target by exchanging either a virtual photon (left) or a Z^0 boson (right).

The scattering amplitude, \mathcal{M} , for the process is a product of current for the electron with the photon or the Z^0 propagator and the hadron current:

$$\mathcal{M}_\gamma = j_\mu \left(\frac{1}{q^2} \right) J^\mu; \quad \mathcal{M}_Z = j_\mu \left(\frac{1}{M_Z^2} \right) J^\mu. \quad (8)$$

The cross sections for scattering right- and left-handed electrons off an unpolarized target are proportional to the square of the total amplitudes:

$$\sigma^r \propto (\mathcal{M}_\gamma + \mathcal{M}_Z^r)^2, \quad \sigma^l \propto (\mathcal{M}_\gamma + \mathcal{M}_Z^l)^2, \quad (9)$$

where only a longitudinally polarized electron beam was considered and \mathcal{M}_Z^r and \mathcal{M}_Z^l represent amplitudes for the incident right- and left-handed electrons, respectively. The parity-violating asymmetry may be expressed as [19]

$$A_{LR} \equiv \frac{\sigma^r - \sigma^l}{\sigma^r + \sigma^l} = \frac{(\mathcal{M}_\gamma + \mathcal{M}_Z^r)^2 - (\mathcal{M}_\gamma + \mathcal{M}_Z^l)^2}{(\mathcal{M}_\gamma + \mathcal{M}_Z^r)^2 + (\mathcal{M}_\gamma + \mathcal{M}_Z^l)^2} \approx \frac{\mathcal{M}_Z^r - \mathcal{M}_Z^l}{\mathcal{M}_\gamma}. \quad (10)$$

Thus, measuring the parity-violating asymmetry gives access to the weak neutral current in a ratio of amplitudes rather than the square of this ratio, greatly enhancing its relative contribution. The size of the asymmetry can be *estimated* based on the ratio of the propagators:

$$A_{LR} \approx \frac{Q^2}{M_Z^2} \approx 360 \text{ ppm at } \langle Q^2 \rangle = 3 \text{ GeV}^2 \quad (11)$$

with $M_Z = 91.2 \text{ GeV}$ [2], a very large asymmetry for a parity violation experiment.

Following this formalism, derived by Cahn and Gilman [19], the parity-violating asymmetry for scattering longitudinally polarized electrons from an unpolarized isoscalar target such

as deuterium (assuming isospin symmetry – this assumption will be discussed in Sec. 4.4) is given by [19, 20]

$$A_d = \frac{\sigma_L - \sigma_R}{\sigma_L + \sigma_R} \quad (12)$$

$$= - \left(\frac{3G_F Q^2}{\pi\alpha 2\sqrt{2}} \right) \frac{(2C_{1u} - C_{1d}) [1 + R_s(x)] + Y(2C_{2u} - C_{2d})R_v}{5 + R_s(x)}. \quad (13)$$

Here, the kinematic variable Y is defined as

$$Y = \frac{1 - (1 - y)^2}{1 + (1 - y)^2 - y^2 \frac{R_{LT}}{1 + R_{LT}}} \quad (14)$$

with $y = \nu/E$ and $\nu = E - E'$ is the energy lost by an incident electron of energy E scattering to an electron of energy E' . The ratio $R_{LT} = \sigma_L/\sigma_T \approx 0.2$ depends on x and Q^2 . The ratios $R_s(x)$ and $R_v(x)$ depend on the parton distribution functions¹:

$$R_s(x) = \frac{s(x) + \bar{s}(x)}{u(x) + \bar{u}(x) + d(x) + \bar{d}(x)} \quad (15)$$

and

$$R_v(x) = \frac{u_v(x) + d_v(x)}{u(x) + \bar{u}(x) + d(x) + \bar{d}(x)}. \quad (16)$$

As described in the introduction, $C_{1u(d)}$ represents the axial Z -electron coupling times the vector Z - u quark (d quark) coupling, while the $C_{2u(d)}$ is the vector Z -electron coupling times the axial Z - u quark (d quark) coupling.

In an approximation of moderately large- x , where sea quark contributions vanish, $R_v \approx 1$ and $R_s \approx 0$. Using $\sin^2 \theta_W \approx 0.23$ for C_{1u} , C_{1d} , C_{2u} and C_{2d} from above,

$$A_d \approx 10^{-4} Q^2 (0.73 + 0.12Y), \quad (17)$$

where Q^2 is in GeV^2 . The sensitivity to $\sin^2 \theta_W$ is approximately given by

$$\frac{\delta \sin^2 \theta_W}{\sin^2 \theta_W} \approx \left(\frac{\delta A}{A} \right) \frac{1 + 0.2Y}{1 + 1.8Y}. \quad (18)$$

¹ Charmed quark contributions may be considered in the same manner as strange quarks; but their contribution is quite small.

2.2. Exploring New Physics Beyond the Standard Model

Since the SLAC E-122 experiment [14, 15], other experiments have succeeded in verifying the electroweak sector of the Standard Model to within a few parts per thousand. Still, there are numerous reasons to believe that what is known as the Standard Model is only part of a larger framework. PVDIS involves exchange of Z^0 between electrons and quarks and thus is sensitive to physical processes that might not be seen in purely leptonic observables, such as the precision A_{LR} at SLC and A_{FB}^l at LEP. There is currently a three standard deviation disagreement [3, 4] in $\sin^2 \theta_W$ between purely leptonic and semi-leptonic observables at the Z -pole from SLC and LEP. The recent NuTeV [6] result on $\sin^2 \theta_W$ at low Q^2 involves a particular set of semi-leptonic charged and neutral current reactions and disagrees with the Standard Model prediction by three standard deviations. A precision measurement of PVDIS will provide a clean semi-leptonic observable to the world data below the Z -pole and will provide essential clues as to the source of these discrepancies.

A precision PVDIS measurement would examine the Z coupling to electrons and quarks at low Q^2 far below the Z -pole. PVDIS is sensitive to a particular combination of couplings and has different sensitivities to extensions of the Standard Model than other semi-leptonic processes (*e.g.*, Qweak). For example, a large axial quark coupling could cause the NuTeV effect, but cannot be seen in C_{1q} . Quark and lepton compositeness is accessible only through C_{2q} but not C_{1q} if a particular symmetry, SU(12), is respected [21]. PVDIS will significantly strengthen the constraints on these possible extensions to the Standard Model. This section describes how PVDIS can explore physics beyond the Standard Model in a complementary way to Atomic Parity Violation [5], JLab QWeak [8], SLAC E-158 Møller [7] and Fermilab NuTeV [6]. Special attention is paid to extensions to the Standard Model to which the C_{2q} couplings are sensitive, as these are unique to PVDIS. A few possible models for new physics that can be probed via measurement of A_d and C_{2q} 's are discussed, including the search for extra neutral gauge boson Z' , compositeness and leptoquark, and super-symmetry (SUSY).

Frequently proposed experiments are characterized by a “mass scale” for which they are sensitive to physics beyond the Standard Model. This can be estimated by considering the low energy effective electron-quark Lagrangian. In analogy to Eqs. (25-27) and (29) of Erler, Kurylov and Ramsey-Musolf [22], the approximate mass scale reached by this experiment

would be [23]

$$\frac{\Lambda}{g} = \frac{1}{\sqrt{2\sqrt{2}G_F} \delta(2C_{2u} - C_{2d})} \approx 1.5 \text{ TeV}. \quad (19)$$

In the following sections we will review possible New Physics search from PVDIS given in literature, including recent development on possible constraints on SUSY.

2.2.1. Z' Searches

Neutral gauge structures beyond the photon and the Z boson (*i.e.* the Z') have long been considered as one of the best motivated extensions of the Standard Model [2]. They are predicted in most Grand Unified Theories (GUT) and appear in superstring theories. While there may be many such states near the Planck scale, many models predict a Z' near the weak scale $M_{weak} \sim 250 \text{ GeV}$.

A Z' which couples to Z^0 will strongly affect the observables around the Z -pole, which have been measured to a remarkable precision. Direct searches at Fermilab have ruled out any Z' with $M_{Z'} < M_Z$ but a heavier Z' (most likely above $\approx 600 \text{ GeV}$) is possible. Such Z' can arise in E_6 [24], a rank-6 group and a possible candidate for the GUT. This E_6 breaks down at the Planck scale and becomes the $SU(3)_C \times SU(2)_L \times U(1)_Y$ symmetry of the familiar Standard Model. The breaking of E_6 to the Standard Model will lead to extra Z 's and it is possible that at least one of these is light enough to be observed. The effect of Z' in E_6 might be observed in ν -DIS, PV e-N scattering, PV Møller scattering and APV [25].

2.2.2. Compositeness and Leptoquarks

If quarks and leptons have intrinsic structure (compositeness), then there may be interchange of fermion constituents at very short distances [1]. The lowest dimension contact interactions are the four-fermion contact interactions between quarks and leptons, described by 8 relevant terms $\bar{e}_i \gamma_\mu e_i \bar{q}_j \gamma^\mu q_j$ where $i, j = L, R$ and $q = u, d$ [26]. These lead to the following shifts in the couplings:

$$\delta C_{1q} = \frac{1}{2\sqrt{2}G_F} (\eta_{RL}^{eq} + \eta_{RR}^{eq} - \eta_{LL}^{eq} - \eta_{LR}^{eq}) \quad (20)$$

$$\delta C_{2q} = \frac{1}{2\sqrt{2}G_F} (-\eta_{RL}^{eq} + \eta_{RR}^{eq} - \eta_{LL}^{eq} + \eta_{LR}^{eq}). \quad (21)$$

where $\eta_{\alpha\beta}^{eq}$ correspond to the extra contributions from new physics to the reduced amplitude $M_{\alpha\beta}^{eq}$ of the Standard Model [27]. These extra contributions are often expressed as $\eta_{\alpha\beta}^{eq} = \epsilon(4\pi)/\Lambda_{eq}^2$ where $\epsilon = +1$ or -1 corresponds to constructive or destructive contribution to the SM amplitude, respectively, and Λ_{eq} is the mass scale of the extra contribution.

In theories that predict quark and lepton compositeness, there are new strong confining dynamics at a scale Λ . Any contact terms produced by the strong dynamics will respect its global symmetries, and it is not difficult to find such global symmetry (other than parity) which ensure cancellations in δC_{1q} 's. For instance, an approximate global SU(12) acting on all left handed first generation quark states will have no effect on C_{1q} 's while still allowing a non-zero contribution to C_{2q} 's ($LL = -LR$ and $RL = -RR$) [21]. Therefore, measurement of C_{2q} 's will provide a unique opportunity to explore quark and lepton compositeness if SU(12) is respected. Using the formalism of Ref. [25], a four-fermion contact interaction of form

$$L_1 = \pm \frac{4\pi}{\Lambda_1^2} \bar{e}_L \gamma^\mu e_L \bar{q}_L \gamma_\mu q_L \quad (22)$$

will change C_{2q} 's by

$$\delta C_{2q} \approx \pm \frac{\sqrt{2}}{G_F} \frac{\pi}{\Lambda_1^2} . \quad (23)$$

Thus the measurement on C_{2q} 's proposed here will set a mass scale limit of $\Lambda_1 > 5.0$ TeV. Although this is somewhat lower than other mass limits [27, 28] where the most recent HERA data [29, 30] are included, all these limits were obtained by only allowing one contact term at a time with all others set to zero. Ultimately, these LL, LR, RL, RR terms must be allowed to vary simultaneously and the results from the proposed measurement will have a different sensitivity to them and thus provide an important input to these fits.

Leptoquarks are vector or scalar particles carrying both lepton and baryon numbers. Leptoquarks can be characterized by

$$\eta_{\alpha\beta}^{eq,LQ} = -\frac{1}{2} \frac{\lambda^2}{M_{LQ}^2} \left(1 + \frac{q^2}{M_{LQ}^2} + \dots \right) \quad (24)$$

where $\eta_{\alpha\beta}^{LQ}$ again is the extra contribution due to leptoquarks to the reduced amplitude $M_{\alpha\beta}^{eq}$ of the SM, M_{LQ} is the mass of leptoquark and λ is its coupling to electron and quarks. For PVDIS, the existence of leptoquarks will change the observed C_{iq} by an amount $\eta_{\alpha\beta}^{LQ}/(2\sqrt{2}G_F)$. Hence a deviation of the measured C_{2q} from its Standard Model prediction can be interpreted as caused by leptoquarks and can set constraint on the leptoquark

properties λ and M_{LQ} . Assuming for simplicity creation of a scalar leptoquark from interactions with u quarks but not d quarks, the measurement proposed here will set a limit of $\lambda_s \leq 0.1(M_{LQ}/100 \text{ GeV})$, comparable to the current limit from the Cs APV experiment.

2.2.3. Supersymmetry (SUSY)

Supersymmetry (SUSY) is a symmetry between bosons and fermions [31]. It requires a Lagrangian which is invariant under transformations which mix the fermionic and bosonic degrees of freedom. In any supersymmetric scheme, all particles fall into supermultiplets with at least one boson and one fermion having the same gauge quantum numbers. Hence, to each fermion and to each vector boson of a gauge theory there will correspond superpartners. If the symmetry were unbroken, the pairs of bosons and fermions would have the same mass – in contradiction with experimental results. Thus if they exist, one must assume heavy masses (above TeV range) because no supersymmetric particles have ever been detected.

Although no supersymmetric particle has yet been discovered, there exists strong motivation for believing that SUSY is a component of the “new” Standard Model. For example, the existence of low-energy SUSY is a prediction of many string theories; it offers a solution to the hierarchy problem, providing a mechanism for maintaining the stability of the electroweak scale against large radiative corrections; it results in coupling unification close to the Planck scale; and more excitingly it can be extended to gravity (the extended version including gravity is called supergravity). In light of such arguments, it is clearly of interest to determine what insight about SUSY the new PVDIS measurements might provide.

The simplest supersymmetric extension of the SM is the Minimal Supersymmetric Standard Model (MSSM). In MSSM, it is possible to have baryon and lepton number violation interactions. However, one outcome of such interaction is rapid proton decay which conflicts with present bounds on the proton lifetime. One way to eliminate such process is to define a new symmetry called R -parity, defined by conservation of the quantum number

$$P_R = (-1)^{3(B-L)+2s} , \quad (25)$$

where s is the spin, B and L are the baryon and lepton numbers of the particle, respectively. All SM particles have $P_R = +1$ while all the superpartners have $P_R = -1$. If R -parity is an

exact symmetry, then no rapid proton decay can occur via B and L violating interactions in MSSM.

The exact conservation of R -parity has many consequences. For low-energy processes involving only SM particles in the initial and final states – such as PVDIS – supersymmetric contributions appear only at loop-level (*i.g.*, virtual superpartners are pair produced). However, one may relax the constraints of R -parity conservation while preserving proton stability by forbidding B violating interactions. In this case, tree level SUSY contributions to low energy processes appear through R -parity violating (RPV) interactions. The effect of SUSY on the coupling coefficients $C_{1,2u(d)}$ in the loop correction and in RPV are discussed in Ref.[?]. Here we use Fig. 4 (taken from Ref.[?]) to illustrate the sensitivity of $A_{PV}^{eD, \text{DIS}}$ to the effects of MSSM loop contributions and tree-level R -parity violation effects [32] compared to those in Q_W^e and Q_W^p . The interior of the truncated ellipse gives the 95% C.L. region from

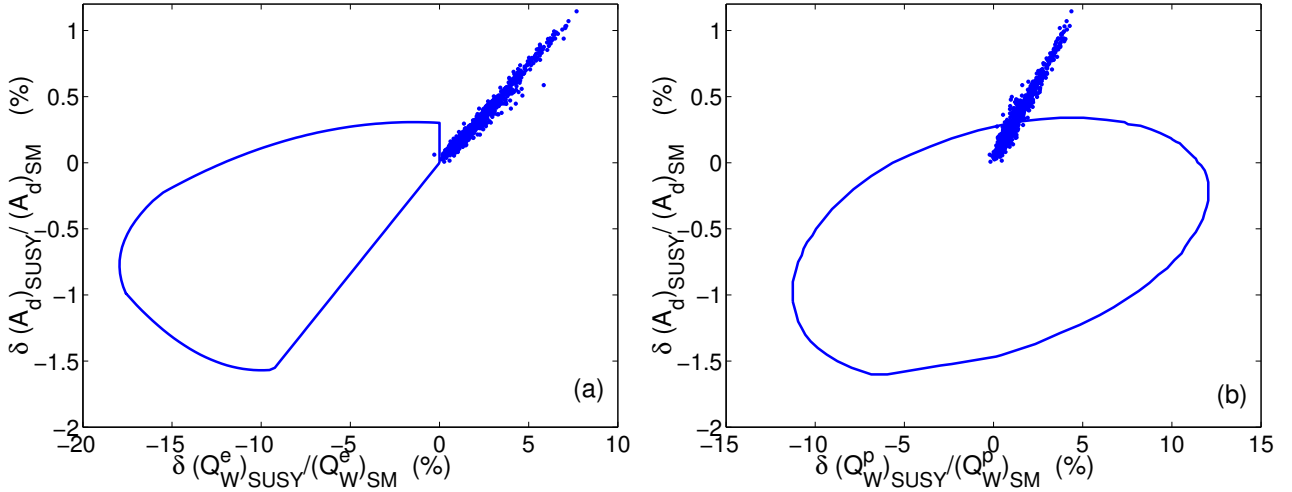


FIG. 4: 95 % CL allowed region for RPV contribution to $A_{PV}^{eD, \text{DIS}}(y = 1, Q^2 = 3.7 \text{ GeV}^2)$ vs. electron weak charge (left) and proton weak charge (right). The dots indicate the SUSY loop corrections.

RPV effects allowed by other precision electroweak data. A deviation of about 1% could be expected from MSSM loop effects while the maximum correction from RPV effects would be -1.5% , corresponding to about 2σ for the precision of the proposed measurement. The presence of RPV effects would induce negative relative shifts in both $A_{PV}^{eD, \text{DIS}}$ and Q_W^e , whereas the relative sign of the loop corrections is positive in both cases. A sizable positive shift in Q_W^p (up to 3σ for the proposed Qweak measurement) due to RPV contributions could

correspond to a tiny effect on $A_{PV}^{eD, \text{DIS}}$ whereas a substantial negative shift in the proton weak charge could also occur in tandem with a substantial negative correction to $A_{PV}^{eD, \text{DIS}}$. On the other hand, even a result for Q_W^p consistent with the SM would not rule out a sizable effect on $A_{PV}^{eD, \text{DIS}}$. Overall, the addition of an eD DIS measurement would provide a useful complement to the PV ee (Møller) and elastic ep (Qweak) measurements, assuming it can be performed with $\sim 0.5\%$ precision or better.

3. EXPERIMENTAL CONFIGURATION AND SYSTEMATIC UNCERTAINTIES

The 12 GeV upgrade to the CEBAF accelerator will vastly increase the kinematics accessible to DIS experiments at Jefferson Laboratory. From the formalism developed in Sec. 2.1, it is clear that the interpretation of these measurements depends on quark scattering and so must be done with DIS kinematics.² The proposed measurement will run in Hall C with an 85 μA polarized beam on a 40 cm liquid deuterium target. Scattered electrons will be detected in both of the Hall C baseline spectrometers, the HMS and SHMS. As with any parity experiment, tight control must be maintained over various systematic effects. Fortunately, however, the PVDIS asymmetry is relatively large this is relatively easy to achieve compared to other parity experiments. First, this section will describe the measurement, the baseline spectrometers and rates. Then, the basic instrumentation and the systematic uncertainties associated with the measurement of A_d will be discussed, including the beamline, polarimetry, and radiative corrections.

3.1. The Measurement with the 12 GeV Baseline Spectrometers

The choice of kinematics for this experiment must meet several criteria. The most important is that the experiment should measure A_d in the DIS region, namely $Q^2 > 1 \text{ GeV}^2$ and $W^2 > 4 \text{ GeV}^2$. In particular, to be optimized for sensitivity to Standard Model parameters, it is desired to keep Q^2 and W^2 as high as possible. Additional considerations are then focused

² The Res-Parity experiment has proposed studying parity violation in the resonance region. A summary of the additional physics which can be probed can be found in the Res-Parity proposal [33].

on minimizing both statistical and systematic uncertainties in the measured asymmetry or in its interpretation, including rates in the spectrometers, the electron/pion ratio and parton density uncertainties. These criteria could be met by employing the HMS and SHMS spectrometers at 13.5° , with a central momentum of 6.0 GeV in the HMS and 5.8 GeV in the SHMS. The lower central momentum in the SHMS serves to reduce a $W^2 < 4$ tail allowed by the large momentum bite. At these settings, the experiment would have $\langle Q^2 \rangle = 3.3 \text{ GeV}^2$, $\langle W^2 \rangle = 7.3 \text{ GeV}^2$ and $\langle x \rangle = 0.34$. The distribution of rate over these kinematic variables for this configuration is shown in Figures 5-7. A summary of some of the properties of the HMS and SHMS are given in Tab. II. Further details of these spectrometers may be found in Ref. [34, 35, 36]. The total rate in this configuration would provide a statistical precision $\delta A_d/A_d = 0.5\%$ in 672 beam hours (assuming 85 μA beam with polarization equal to 80%).

3.2. Particle Identification and Pion Contamination

Pion rate and PID

The pion rates were calculated using a fit to pion photo-production data of Wiser [37] taken at SLAC. As can be seen from Tab. II, the average π^-/e^- ratio ($R_{\pi/e}$), is relatively small for this measurement. In some regions of each spectrometer's acceptance (the lowest E' values accepted) however this ratio can be greater than 50%. In the SHMS, particle identification will be done by means of a lead-glass shower counter and a 2.5 m long atmospheric pressure Čerenkov counter. The shower counter is expected to have a pion rejection factor of $(1 - 5) \times 10^{-2}$ [34]. Combined with the Čerenkov counter, a pion rejection factor of $\epsilon_{\text{SHMS}} = 1 \times 10^{-4}$ should be achievable. The HMS uses a pressurized Čerenkov counter as well as a shower counter for π^-/e^- separation. This combination has a combined pion rejection factor of $\epsilon_{\text{HMS}} = 1 \times 10^{-4}$.

Pion asymmetry

The asymmetry of pion production in the DIS region is expected to be small. We first discuss the possible effect from single spin asymmetry. The single beam-spin azimuthal asymmetry (beam SSA) reported recently by the HERMES collaboration is consistent with zero [38], but with large error bars. The data from JLAB Hall B show a $A_{LU}^{\pi^+ \sin \phi} \sim 5\%$ azimuthal beam SSA

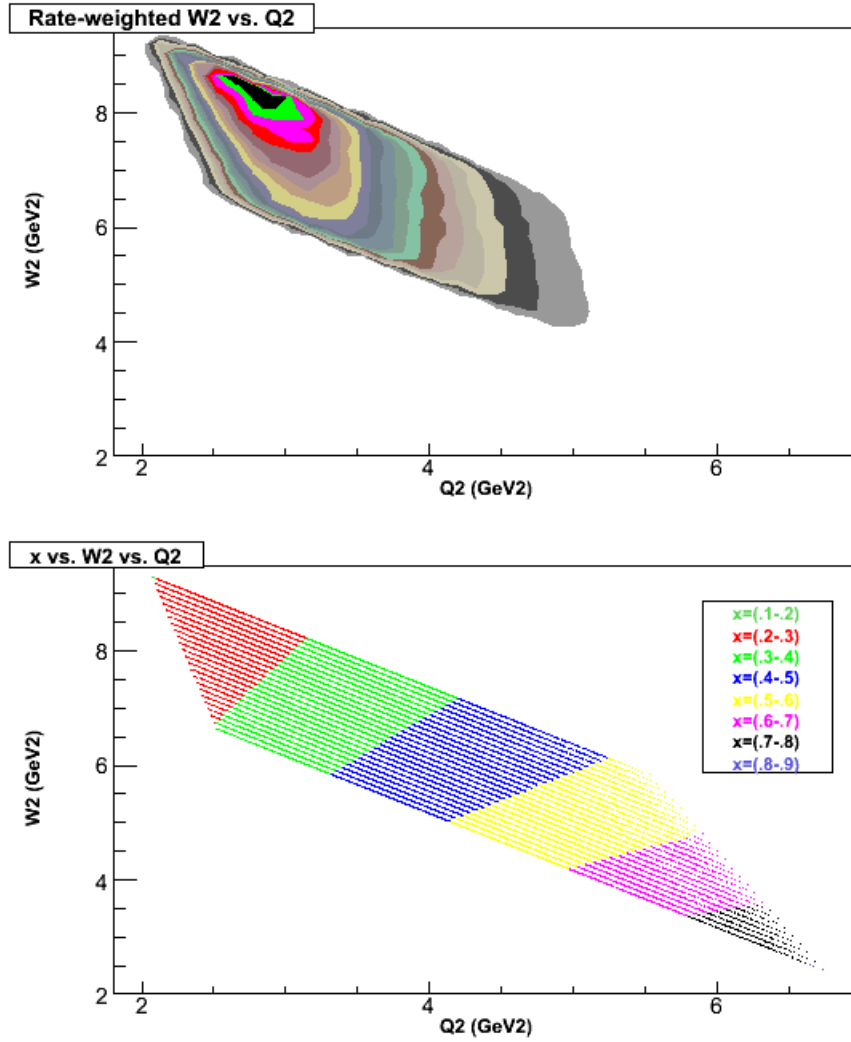


FIG. 5: The approximate kinematic coverage of the HMS spectrometer, configured as proposed, shown as W^2 vs. Q^2 . Top plot: color contours show the rate distribution, modeled with $\pm 10\%$ momentum acceptance. Bottom plot: color bands display ranges of Bjorken x . From left to right (or from top to bottom): $x = (0.2, 0.3)$ (red), $x = (0.3, 0.4)$ (green), $x = (0.4, 0.5)$ (blue), $x = (0.5, 0.6)$ (yellow), $x = (0.6, 0.7)$ (magenta) and $x = (0.7, 0.8)$ (black).

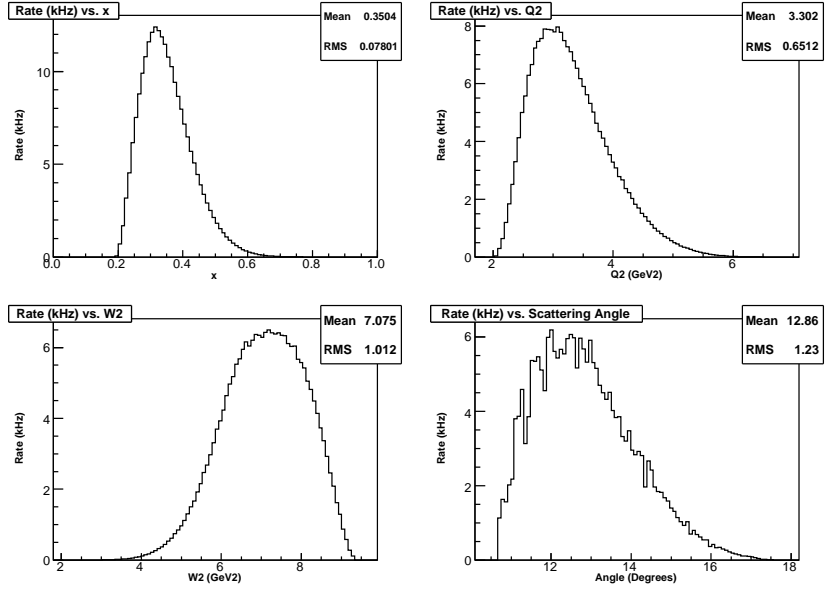


FIG. 6: Rate distribution plotted versus kinematic variables x , Q^2 , W^2 , and lab scattering angle for the assumed acceptance of the HMS spectrometer with central angle 13.5° and central momentum 6.0 GeV.

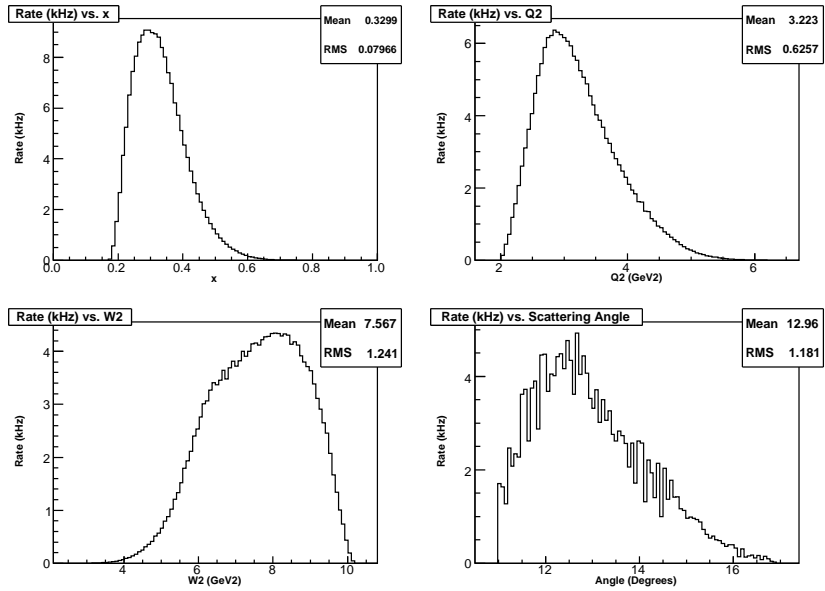


FIG. 7: Rate distribution plotted versus kinematic variables x , Q^2 , W^2 , and lab scattering angle for the assumed acceptance of the SHMS spectrometer with central angle 13.5° and central momentum 5.8 GeV.

TABLE II: This table lists the spectrometer settings, kinematic variables (and their ranges) as well as expected rates for both spectrometers [34, 36]. The combined statistical uncertainty on A_d is 0.5%.

	HMS		SHMS	
	Average	Range	Average	Range
Central Angle	13.5°	-	13.5°	-
Momentum (GeV)	6.0	5.4 – 6.6 (±10%)	5.8	4.9 – 6.7 (−15/ + 15%) ^a
$\delta\Omega$ (msr)	-	6.8	-	3.5
Q^2 (GeV ²)	3.3	2.6 – 4.0 ^b	3.2	2.6 – 3.8
W^2 (GeV ²)	7.1	6.1 – 8.1	7.6	6.3 – 8.8
x	0.35	0.27 – 0.43	0.33	0.25 – 0.41
DIS Rate (kHz)	190		138	
A_d (ppm) ^c	285	220 – 350	280	210 – 340
$\delta A_d/A_d$ [%] (672 hours)	0.65		0.77	
π/e ratio ^d	0.3	0.1 – 0.6	0.45	0.1 – 1.0
e^+/e ratio	0.00031	$2.7 \times 10^{-5} - 0.001$	0.0007	$3.2 \times 10^{-6} - 0.0036$
Total Rate (kHz)	240		202	

^aFor the purpose of this rate estimate a $\pm 15\%$ momentum acceptance was used. A full simulation is underway.

^bThe range for these kinematic variables describes the coverage of the RMS width.

^cThe range gives the variation in the asymmetry over each spectrometers acceptance.

^dThe range of π/e depends on the π or e momentum.

for π^+ electro-production [39]. However, since we are doing an inclusive measurement where the azimuthal angle for the pion in the $\gamma^* - N$ center-of-mass system, ϕ^* , is being integrated, we do not expect any background from SSA [40]. Next, the only possible background to the proposed measurement is coming from weak interactions between partons. Compared to the measured asymmetry, which comes from the interference term between electromagnetic and weak interactions, this background is suppressed by a factor of $100 \sim 1000$. Since the measured asymmetry is about 280 ppm, the maximum background one can have is less than

1 ppm. Overall, we expect that the effect on A_d^{PV} from pion asymmetry to be well below 10^{-4} .

In addition, the pion asymmetry A_d^π will be measured at the same time as A_d simply by requiring a pion rather than rejecting it, with fewer statistics since $R_{\pi/e} < 1$. This will lead to a determination of $\delta A_d^\pi \approx 3$ ppm. Assuming the worst case, $\epsilon \approx 10^{-3}$ and $R_{\pi/e} \approx 1$, the uncertainty due to pion contamination is given by

$$\left. \frac{\delta A_d}{A_d} \right|_{\pi \text{ contam.}} = \epsilon R_{\pi/e} \left(\frac{\delta A_d^\pi}{A_d} \right) \approx 1.1 \times 10^{-5}, \quad (26)$$

which is a negligible amount.

3.3. Pair Production Background

Part of the background of the proposed measurement comes from the pair production $\gamma \rightarrow e^+ + e^-$, where γ is coming from the decay of the electro- and photo-produced pions. Usually the e^+e^- pairs are assumed to be symmetric and the asymmetry of the e^- of the pair production background is the same as the positron asymmetry, while the latter can be measured by reversing the polarity of the spectrometers. To ensure that the proposed measurements are not affected by this background, we would like to control the uncertainty due to e^+ to 1×10^{-3} , or $0.2\delta A_{e^-}$ where $\delta A_{e^-} = A_d \times 0.5\%$ is the expected statistical uncertainty. Thus the positron asymmetry needs to be measured to $\alpha\delta A_{e^+} = 0.2\delta A_{e^-}$ where α is the fraction of the electrons contributed from the pair production to the total electron yield. The statistics required is therefore

$$N_{e^+} = \frac{1}{(\delta A_{e^+})^2} = \frac{1}{\left(\frac{0.2}{\alpha}\delta A_{e^-}\right)^2} = \frac{25\alpha^2}{N_{e^-}} \quad (27)$$

The beam time required to reach this statistics is

$$T_{e^+} = \frac{N_{e^+}}{\text{rate}_{e^+}} = \frac{N_{e^+}}{\alpha \text{rate}_{e^-}} = \frac{25\alpha N_{e^-}}{\text{rate}_{e^-}} = 25\alpha T_{e^-} \quad (28)$$

For the proposed measurement we used a conservative estimate using the Wiser fit [37] for the π^0 and found $\alpha = 0.0003$ for the HMS and 0.0007 for the SHMS averaged over the acceptance. We will use the regular DAQ to measure the real positron rate with reversed spectrometer polarity. Then we will use the fast counting DAQ (see section 3.8) to measure the positron asymmetry to the desired level. The request beam time is 12 hours.

3.4. Rescatter Background

The rescattering of high-energy electrons or pions from the walls of the spectrometer creates a potential source of background for the proposed measurement. This “rescattering” background, which is typically rejected using a combination of tracking and particle identification in low-rate experiments without difficulty, must be treated carefully in this high-rate measurement due to the limited information available in each event.

The magnitude of this effect will be combination of the probability for products of this scattering in the spectrometer to reach the detectors and the effectiveness of the detector/DAQ package to distinguish those tracks from tracks originating in the target. A detailed analysis of this possible problem will require a careful simulation of the spectrometer and detector geometry. Measurements will be taken with a low beam current (to allow the use of the tracking chambers and the standard DAQ) to study this small background and verify the accuracy of the simulation.

We also intend to directly estimate the rescattering contribution using both direct measurements and a “pseudo-simulations” method. The direct method includes a series of dedicated measurements with a hydrogen target at lower beam energy. At a beam energy of 6.6 GeV, the spectrometer will be tuned to place the hydrogen elastic peak at various points inside the spectrometer. The detected rate will be used to estimate the “rescattering probability”: the probability that an electron, interacting at a given point in the spectrometer, produces a count in the production DAQ. At this beam energy, the spectrometer optics will be similar to that used in the production running. Therefore, the rescattering probability can be convoluted with the electron flux distribution to estimate the total count-rate contribution from interactions in the walls of the spectrometer during production running. We plan to use a shorter (20 cm) LH₂ target for this study, as the electron rescattering probability is most cleanly measured with a reduced radiative tail. Table III shows the running conditions for elastic scattering. This empirical measure of the contribution of electron interactions with the spectrometer walls also serves to cross-check the simulation, which must still be used to estimate the rescattered contribution from pions.

The rescattering contribution from electrons was studied in this way by the HAPPEX collaboration (HAPPEX-H: E99-115 and HAPPEX-He: E00-114) [41]. These experiments

used an analog-integrating detector, and therefore had no method for excluding rescattered background particles. The experiment used the Hall A High Resolution Spectrometers. In those measurements, the rescattering probability was around 1% for momenta near to the central momenta (within a few percent of $\delta p/p$). This probability rapidly dropped to 10^{-5} for interactions with the spectrometer wall took place before the last spectrometer quadrupole element. For HAPPEX-Helium, the rate of quasi-elastic scattering from the Helium target which was steered into the spectrometer walls was several times the elastic signal rate, leading to a rescattering in the focal plane on order 0.2% of the detected elastic rate. It is reasonable to expect that the detected rescattering signal in the proposed measurement will also form a dilution at the few 10^{-3} level. Factors that would argue for a larger contribution, such as the continuous DIS momentum distribution and the relatively open spectrometer geometry, will be counteracted by the ability to exclude background through position, energy, or PID information from the fast counting DAQ.

To confirm this expectation, we are also trying to perform a “pseudo-simulation” using the same method as the 6 GeV PVDIS experiment in Hall A. In preparation for the 6 GeV experiment, we are using data from a previous 6 GeV DIS experiment (E99-117 [42]) where the PVDIS trigger algorithm was added at the software-level using the non-calibrated ADC

TABLE III: Running configuration for elastic scattering on a 20 cm LH₂ target to measure the re-scattering background. Also shown are the rate estimates for a 10 μ A beam current for the two spectrometers. The spectrometer central momentum scanning range allows the elastic peak to fall as much as 10% outside the nominal acceptance and can be extended further, and the beam current can be higher than 10 μ A when the elastic peak is outside the acceptance. We expect to spend 1 day of beam time for this measurement to allow a thorough study of the re-scattering probabilities on-line at various kinematic points.

E_{beam}	Spectrometer	Elastic	HMS, SHMS	HMS, SHMS
(GeV)	central	E_p	elastic rate	central
	angle	(GeV)	at 10 μ A (Hz)	momentum
				range (GeV/c)
6.6	13.5°	5.5	8.0K, 3.8K	4.0-7.0, 3.4-7.5

signals from the Cerenkov detector, lead glass counters and the scintillators; and a direct comparison of the PVDIS trigger and the regular DAQ using vertical drift chambers (VDC) is possible. Effects of electrons from nearby DIS and the resonance region can be studied by requiring the reconstructed track to be off-central or to fall outside the nominal acceptance of the spectrometer. Our first “pseudo-simulation” shows that the fraction of these outside-acceptance events is very small, at the $< 0.5\%$ level. Currently we are still working on this analysis because some modifications to the Hall A VDC tracking algorithm are required for this purpose. But combining the already small fraction we found, and the fact that DIS re-scattered electrons have very similar asymmetry to the primary measurement, the dilution effect from re-scattered electron background is expected to be fairly small, if not negligible. A similar study using the two Hall C spectrometers will be performed to make sure the rescattering background is under control.

One also have background from pion rescattering. However, pions can be rejected by PID detectors reliably and will only have negligible contribution to the primary measurement. In Hall A again this has been studied via a “pseudo-simulation” and the DIS data we used had much higher π/e ratio (about 30/1) than our proposed measurement. Results from this “pseudo-simulation” show that even though only non-calibrated ADC signals can be used to form the PVDIS trigger, a pion contamination factor of 10^{-4} can be achieved without difficulty and can be reduced further by adjusting discriminator thresholds.

Overall, we expect that the total rescattering rate to be at most at a few $\times 10^{-3}$ level. And among these re-scattered events, resonance electrons and pions will only consist a small fraction. The re-scattered DIS electrons may be the majority of these re-scattering events but they have very similar kinematics and Q^2 to the primary measurement thus will only introduce a very small dilution. Therefore we expect the total uncertainty due to the rescattered background to be in the 10^{-4} range.

3.5. Polarized Electron Source

Parity-violation experiments are typically very sensitive to the problem of misinterpreting a helicity-correlated asymmetry on the beam as a parity-violating physics asymmetry. For this reason, it is necessary for such experiments to carefully control helicity-correlated

asymmetries on the electron beam. Previous collaborations on parity-violation experiments have worked closely with the source group to develop an understanding of the sources of intensity and position asymmetries on the beam and techniques for suppression of these effects. Careful configuration techniques and active feedback has suppressed both helicity-correlated intensity and position differences at a level well beyond that which is required for this proposal. In particular, helicity-correlated beam differences were suitably controlled for the HAPPEX-H measurement. That measurement was made at a very forward angle, in which requirements were about an order of magnitude more stringent than the proposed experiment. In addition, the upcoming PREX [43] experiment in Hall A and QWeak [8] experiment in Hall C, which will run at beam energies around 1 GeV, will demand control of helicity-correlated beam asymmetries at a level 2-3 orders of magnitude beyond what would be required for this proposal.

It is therefore expected that established techniques will suitably control helicity-correlated beam differences. These techniques will be applied in collaboration with the Electron Gun Group and CASA beam physicists.

3.6. Beam Line and Polarimetry

The rates and beam allocations in this proposal assume an 11 GeV beam at 85 μA of current with 80% polarization. An uncertainty of 0.1% in the absolute energy of the electron beam from arc measurements in Hall C is expected to be easily achieved with an 11 GeV beam [34]. This should be controlled as tightly as possible, since this uncertainty feeds into the Q^2 uncertainty and hence the extracted value of $\sin^2 \theta_W$ and $2C_{2u} - C_{2d}$ (see Sec. 3.9). If necessary, a raster as large as 3 mm \times 3 mm may be used to reduce correlated noise from target boiling.

The physics goals of this proposal require state-of-the-art electron beam polarimetry. This is recognized as one of the leading experimental challenges and will be a focus of effort by the lead institutions. The experiment will employ both Møller and Compton polarimeters in Hall C. The Basel Møller polarimeter [44] will be upgraded for operation at 11 GeV and is expected to maintain its accuracy, now quoted at $\sim 0.5\%$ (absolute). Unfortunately, this device will presently only work at low current (a few μA), leaving open the possibility of

a current-dependent polarization shift. Techniques for extending this to a few 10's of μA have been developed in preparation for the QWeak experiment, but these may not be easily applicable to higher beam energies. Since the Møller polarimetry technique is invasive, it will also require interpolation between periodic measurements, which provides an additional source of systematic uncertainty.

Compton polarimetry is a very promising technique for sub-1% polarimetry at few GeV beam energy. Compton polarimetry is non-invasive and operates at high beam currents, so it can be employed as a continuous polarization monitor. The polarization of the photon target can be measured to very high precision, and intrinsic sources of systematic uncertainties are very small. (By comparison, knowledge of intrinsic phenomena like the Levchuck effect in Møller polarimetry [45] or the Sherman function in Mott polarimetry [46] may ultimately limit the precision of those techniques.) In addition, the polarization results deduced from the independent measurement of the Compton-scattered photons or Compton-scattered electrons share a limited set of systematic errors, which in past experience have been sub-dominant. Thus careful Compton polarimetry involving independent electron and photon analyses provides a robust, internal cross-check. A Compton polarimeter at SLAC SLD [47] operating with a 46 GeV electron beam has already achieved a polarization measurement with a total uncertainty of 0.5%. As an indication of the potential of this method, it is worth noting that a 0.3% Compton polarimeter was previously proposed in support of a PVDIS measurement at SLAC (the measurement was ultimately not approved) and as a development for the ILC. In general, Compton polarimetry is easier at higher beam energies where the analyzing power is larger. The achievements of the Hall A Compton polarimeter, utilizing an infrared Fabry-Perot cavity, are therefore particularly encouraging. The recently published results of the HAPPEX experiment quote a polarimetry uncertainty of 1% at a beam energy around 3 GeV [48]. The Hall A Compton polarimetry is currently being upgraded to use a green laser in preparation for the PREX experiment, and even better precision is expected once this upgrade is complete.

A Hall C Compton polarimeter is being developed in preparation for the upcoming QWeak experiment. Although optimized for performance at beam energies near 1 GeV, this polarimeter will be reconfigured for use at 11 GeV by reducing the chicane deflection. It is reasonable to expect a significant improvement over the 1% HAPPEX polarimetry result

for the planned Hall C polarimeter operating at 11 GeV. Both the analyzing power and the momentum separation of the Compton scattered electrons will be increased by the higher electron beam energy and the use of green (532 nm) laser light. The Hall C polarimeter will utilize a single-pass pulsed laser in place of a resonant cavity, which should allow for continuous monitoring and improved precision on the measurement of the laser light polarization. There will also be more experience at the laboratory in high-precision Compton polarimetry. The upcoming PREX and QWeak experiments, which will run at beam energies near 1 GeV, require high-current polarimetry at a precision of approximately 1%. Given the particular difficulty of such low-energy Compton polarimetry, these measurements will set the stage for sub-1% Compton polarimetry for both Halls A and C at an 11 GeV CEBAF.

One possible problem which will not be resolved until after the energy upgrade regards beam quality. The effect of synchrotron radiation in the arc is expected to increase beam emittance by a factor ~ 30 . In addition to this increased emittance, the beam halo and energy tails may also increase due to a reduction in field uniformity of steering and focussing magnets in the accelerator at high excitations. These changes will increase the difficulty in controlling background rates. It is therefore necessary that beam quality requirements for 11 GeV Compton polarimetry are considered during the design of the energy upgrade of both the accelerator and the Hall C beamline, and it is expected that commissioning of the 11 GeV polarimeter will require close collaboration with accelerator physicists to control background levels.

3.7. Liquid Deuterium Target

Target Impurity

The experiment will use a 40 cm long cryogenic liquid deuterium target, corresponding to 0.055 radiation lengths. This length permits the entire target to be seen by the HMS at 12.5° . The heat load for a $85 \mu\text{A}$ beam on this target is approximately 1.6 kW. This is well under the heat load for the QWeak target [8] and the anticipated target cooling capacity for the post-upgrade Hall C cryo-target system [35]. In the following we will discuss about effects from the impurity of the liquid deuterium, the cell endcaps, and the target density fluctuation under high beam currents.

The liquid deuterium used at Jefferson Lab typically contains [49] 1889 ppm HD, <

100 ppm H₂, 4.4 ppm N₂, 0.7 ppm O₂, 1.5 ppm CO (carbon monoxide), < 1 ppm methane and 0.9 ppm CO₂ (carbon dioxide). Compared to the statistical accuracy of the measurement, all of these contributions are small. The largest contamination to the measured asymmetry would be from the proton in HD. Since the asymmetry of the proton is given by [20]

$$A_p = \left(\frac{3G_F Q^2}{\pi\alpha 2\sqrt{2}} \right) \frac{2C_{1u}u(x) - C_{1d}[d(x) + s(x)] + Y [2C_{2u}u_v(x) - C_{2d}d_v(x)]}{4u(x) + d(x) + s(x)} \quad (29)$$

which is within 20% of the asymmetry of the deuteron, the proton in HD and H₂ contributes a $\delta A_d/A_d < 0.4 \times 10^{-3}$ uncertainty to the measured asymmetry.

Target Endcaps

Since the target cell endcaps are made of material other than deuterium, it may have different PVDIS asymmetries and will introduce a change in the measured asymmetry compared to that of pure deuterium. The best way to reduce this effect is to use light material and make the endcaps as thin as possible, for example a few mils of Be. However, such thin Be windows are very difficult to machine. Another light material that is commonly used, havar, is easy to melt in a 85- μ A beam. Thus we consider here only Al windows. The endcaps of a typical target cell at JLab are made of ≈ 10 mil aluminum in average and the uncertainty on this thickness is ± 0.005 mm [50]. For *G0* experiment a special cell was made with Al endcaps ≈ 5 mil thick. Using the typical 10 mil thickness, the ratio of yield from the two endcaps to that from LD₂ is

$$\eta = \frac{N_{endcap}}{N_{LD2}} = \frac{L_{endcap}}{L_{LD2}} \times \frac{\rho_{endcap}}{\rho_{LD2}} = \frac{10 \text{ mils} \times 2}{40 \text{ cm}} \times \frac{2.7}{0.169} = 2.03\% \quad (30)$$

and $\delta\eta/\eta = 0.02$. Because Al has $Z = 13$, $N = 14$, the asymmetry of \vec{e} -Al DIS is about 4% different from A_d . Assuming the measured asymmetry of the target cell is A_{cell} , then the asymmetry for the deuteron can be extracted as

$$A_d = A_{cell}(1 + \eta) - \eta A_{Al} , \quad (31)$$

with an uncertainty of $\Delta A_{endcap} = \sqrt{(A_{cell}\Delta\eta)^2 + (\eta\Delta A_{Al})^2}$. We can correct for this effect by measuring the PVDIS asymmetry for Al, A_{Al} , using a thick Al cell. Assuming N_{endcap} is number of events coming from the two endcaps of the LD₂ cell, and the uncertainty of the measurement on A_{Al} is ΔA_{Al} and the statistics needed is N_{Al} , Keeping the uncertainty of

this correction to be 0.1% of A_d , we have

$$\begin{aligned}
0.1 \text{ \%} &\geq \frac{\Delta A_{endcap}}{A_d} = \eta \frac{\Delta A_{Al}}{A_d} = \eta \frac{\Delta A_{Al}}{\Delta A_d} \frac{\Delta A_d}{A_d} = \eta \frac{1/\sqrt{N_{Al}}}{1/\sqrt{N_{LD2}}} \frac{\Delta A_d}{A_d} = \eta \frac{\sqrt{N_{LD2}}}{\sqrt{N_{Al}}} \frac{\Delta A_d}{A_d} \\
&= \eta \frac{\sqrt{N_{LD2}}}{\sqrt{\lambda N_{endcap}}} \frac{\Delta A_d}{A_d} = \eta \frac{1}{\sqrt{\lambda \eta}} \frac{\Delta A_d}{A_d} = \sqrt{\frac{\eta}{\lambda}} \frac{\Delta A_d}{A_d} = 0.5\% \sqrt{\frac{2.03\%}{\lambda}}
\end{aligned} \tag{32}$$

where λ is the ratio of the product (Al endcap thickness) \times (production time) of dummy and LD₂ cells. Note that the statistical uncertainty $\Delta A_{d,stat} = 1/\sqrt{N_{LD2}} \approx 0.5\% A_d$ was used in the calculation. Limiting $\frac{\Delta A_{endcap}}{A_d} \leq 0.1\%$ we obtain $\lambda > 0.51$. If we match the radiation length of the thick dummy cell to half of the LD₂, then we need 20 \times thicker (5.1 mm) endcaps and up to 2.5% of the beam time will be spent on the thick dummy cell, or 0.6 days (15 hours) for the proposed measurement. The expected uncertainty on the Al asymmetry is $\Delta A_{Al}/A_{Al} = 5\%$, contributing to an uncertainty of $\Delta A_d/A_d = 0.04\%(\eta) + 0.1\%(\Delta A_{Al}) \approx 1 \times 10^{-3}$ which is dominated by the error on the Al asymmetry. Another approach is to correct for this shift using the calculated asymmetry for $e - Al$ PVDIS instead. Assuming the calculation is good to 10% level (which include all possible effects including new physics, hadronic effects of quarks inside the proton, as well as EMC effects on PVDIS), the calculation will provide a cross check of the endcap correction.

Target Boiling Noise

The dominant concern with cryogenic targets in parity-violation experiments is density fluctuations where localized beam heating creates bubbles in the liquid and causes a rapid jitter in the instantaneous luminosity by changing the target density. Such an effect injects additional noise into the measurement which, if large, can ultimately reduce the statistical precision of the measurement.

In the proposed measurement, the detected rate is around 330 kHz (see Tab. II). The statistical uncertainty on the asymmetry per beam pulse pair (33 ms $H+$ and 33 ms $H-$, 66 ms total) is on the order 6500 ppm. The noise effect should be kept small to cost less than $< 5\%$ of statistical precision; at the proposed rate, this corresponds to density fluctuations of around 2100 ppm. The recent HAPPEX experiment found a noise of level of approximately 250 ppm at 70 μA on a 20 cm LH₂ cell and a 5×5 mm² raster size. If scaled by power density, then a 3×3 mm² raster size is sufficient to control the noise below 2000 ppm at 85 μA for a 40 cm long cell. The noise level for LD₂ is expected to be lower than LH₂ under the

same operating conditions. In addition, the approved HAPPEX-III (E05-109) and QWeak (E05-008) experiments each have much more stringent requirements for target fluctuations. In light of this, we plan to use a $3 \times 3 \text{ mm}^2$ raster and we expect the comparatively loose requirements for this proposal should be easily achieved. Of course, commissioning studies will test for target boiling effects before the running to confirm that these running conditions are sufficient.

Helicity-Correlated Density Fluctuation

An additional concern can be found in the possible coupling of target density to the helicity state of the beam. One example would be a helicity-correlated beam spot size asymmetry, with a target density fluctuation that significantly couples to beam spot size. Such an effect (which has never been observed and remains entirely speculative) would be very dangerous for the high-precision parity-violation experiments such as HAPPEX-III and QWeak. Of necessity, these experiments will establish methods for estimating and reducing both these possible helicity correlations in the electron beam, and any coupling of these beam parameters to target density. These experiments, which will run in the near future, will be forced to develop solutions to these potential problems in order to meet far more stringent requirements on both random noise and helicity-correlated effects.

3.8. Data Acquisition

The requirements for the front end electronics and the data acquisition (DAQ) are determined by the high rate and the need to separate electrons from pions. In Tab. II, the estimated total rate is under 400 kHz. The DAQ currently being designed for the HMS or the SHMS can only count up to 10 kHz [34] thus cannot be used for the proposed measurement and a new DAQ system is needed. As a conservative estimate, the new DAQ should be able to accept rates on the order of twice the expected rate, or up to 1 MHz. The electron/pion separation requirement necessitates the use of a counting rather than an integrating DAQ as used in previous parity violation experiments at JLab. A fast counting DAQ will also be used by the 6 GeV PV-DIS (E05-007) [13] experiment which has similar requirement to the present measurement (total rate $\sim 500 \text{ KHz}$ with a π/e ratio of ≈ 1).

For the proposed measurement we will employ a similar trigger setup as E05-007: For

each spectrometer, we will need to read the hit patterns from the trigger hodoscopes and ADC signals from the Čerenkov and lead glass shower counters. The wire chambers will not be active. Two possible read out methods are being considered: one using an array of scalers to count events, and a second, more sophisticated method using flash ADC's (FADC). Both of these methods will be used for the proposed measurement. In the scaler method, particle identification is determined via preset thresholds on the Čerenkov and shower counters. Prior to production running, these thresholds must be carefully set and then checked for drift during production data collection. The lead glass shower detector will be segmented and blocks in each segment are summed to form a trigger signal. Then trigger signals from all groups is "OR"ed to form the final trigger. Alternatively, trigger signals from each group can be used individually to provide segmentation of Q^2 - or W -bins over the accepted range of kinematics.

In the FADC method, the detector signals (PID and scintillator) would be digitized and then an on-board processor (called "FPGA") would determine the particle identification based on a pre-existing algorithm. Over each helicity pulse (33 ms) the FPGA would keep track of both the total number of electrons and pions separately, and is possible to study electron pile-up events using different algorithms with very high thresholds. In both methods the readout dead time and pileup must be carefully watched. FADC's are currently being developed both commercially (*e.g.* Struck) and in house at JLab (for Hall D). In both cases, the FADC's have resolutions better than 8 bit and sampling speeds greater than 100 MHz. The Hall C SHMS effort is already considering using these units [34]. Little additional effort would be required to equip the HMS scintillators, Čerenkov and shower counters with similar units. To continuously monitor the PID efficiency a prescaled fraction of the events will be read out entirely to be cross-checked with the scaler-based trigger. In a zero-suppressed mode, the FADC/FPGA combination could provide to the VME bus the hodoscope hit pattern (4 bytes), the Čerenkov ADC values (2 bytes) and the above pedestal shower counter ADC values (approx. 8 to 12 bytes) for a total of approximately 16 bytes per event.

The experiment will need to collect data with lower luminosity to study issues related to rate dependencies, electronic dead time, computer dead time and PID efficiency. While traditionally these effects are of major concerns for high rate experiments, and can only be studied using high-frequency pulsers, simulations or luminosity scan, they are of less worry

for the proposed DAQ because the FADCs have, in principle, zero deadtime. Full event sampling of the FADC signals at lower read-out rate, that is, continuous readout at full luminosity with low duty-cycle, will allow fine analysis on an event-to-event basis and thus a precise and reliable determination for all these effects.

Overall, we request for three days of beam time to commission the DAQ, to run at low current and cross-check with the regular DAQ to address PID and background-related issues, and to “scan” from low to high beam currents to study rate dependencies, dead times and pile-ups using the FADC.

Currently the E05-007 collaboration is working on a scaler read-out system partially equipped with FADCs for systematic study for use with the HRS in Hall A. “Pseudo-simulations” using previous DIS data from Hall A have shown good pion rejection efficiency and the reliability of this trigger system in many aspects is being studied now, including the possibility to reject rescattered events as described in previous sections. In summer/fall of 2007 a 2/3 setup for the Right HRS in Hall A will be assembled and tested in the EEL building, and in 2008 will be moved into the Hall for parasitic testing. Eventually, the 6 GeV PVDIS DAQ will be thoroughly tested at rates of 500 kHz during its running. With more development on the FADC being carried out, we expect that the 12 GeV DAQ setup, which will be based on a similar approach but also fully equipped with FADCs, to be able to handle the higher rates with the tighter precision requirements of this proposal.

3.9. Determination of Q^2

Since the measured asymmetry is proportional to Q^2 , this uncertainty will feed directly into any interpretation of the measured asymmetry. Thus, the uncertainty in the measured kinematics will act as an error on the reported asymmetry A_d . The Q^2 is calculated from $Q^2 = 2EE'(1 - \cos \theta)$. The uncertainty in the beam energy from arc measurements will be $\delta E/E = 1 \times 10^{-3}$ [34]. The uncertainty in the scattered electron’s energy as measured by the HMS or SHMS is $\delta E'/E' = 1 \times 10^{-3}$ [34]. The nominal angular resolution of the pointing of the SHMS is 0.003° , or $\delta \theta = 0.17$ mrad [34]. For the HMS, previous measurements in Hall C have achieved $\delta \theta = 0.4$ mrad [51].

For the proposed measurement, it will be necessary to calibrate the Q^2 acceptance at low

luminosity using the standard spectrometer tracking detectors. The E' and θ acceptance of the new FADC/scaler-based DAQ system will be slightly different than that of the standard spectrometer triggers, so it will be necessary to study the kinematic acceptance by triggering the standard spectrometer DAQ using the fast-counting DAQ trigger, at low beam currents. The kinematic acceptance for the FADC/scaler-based trigger can then be measured precisely using tracking information from the regular DAQ. In addition, the rate dependence of the Q^2 acceptance will also be studied using the FADCs in scans up to full luminosity, in a mode with continuous readout periods but a low duty-cycle. This zero dead-time cross-check allows verification that rate dependent effects do not modify the kinematic coverage, through some error in DAQ design or implementation.

A Monte Carlo simulation will be used to correct for the non-linearity of the asymmetry over the accepted range of Q^2 , thus allowing the measured asymmetry to be interpreted as corresponding to a single average Q_{avg}^2 . As in previous parity-violation experiments, this correction will introduce negligible systematic uncertainty relative to the uncertainties due to spectrometer pointing. Combining these effects (using $\delta\theta = 0.4$ mrad for both the HMS and the SHMS) gives $\delta Q^2/Q^2 = 3.9 \times 10^{-3}$.

3.10. Radiative Corrections

Electromagnetic Radiative Corrections

Figure 3 describes the scattering process at tree level. In reality both the incident and the scattered electrons can emit photons. Consequently when we extract cross sections and asymmetries from the measured values there are electromagnetic radiative corrections to be made. The theory for the EM radiative correction was first developed in the late 1970's [52]. The correction can be calculated and the uncertainty in the correction is mainly due to the uncertainty of the structure functions (F_2 and R for an unpolarized target) that are used in the calculation.

The ratio of the radiated (observed) cross section and asymmetry to the un-radiated (Born) ones has been calculated [53] and the uncertainty in the asymmetry correction was found to be at the 0.4% (relative) level, corresponding to an uncertainty of < 0.004 for $(2C_{2u} - C_{2d})$ and an uncertainty of 0.002 to $\sin^2 \theta_W$ for the proposed measurement.

Electroweak Radiative Corrections

The products of weak charges $C_{1,2u(d)}$ given by Eq. (1-4) are valid only for the case in which there is no electroweak radiative correction. With this correction they are given by

$$C_{1u} = \rho' \left[-\frac{1}{2} + \frac{4}{3}\kappa' \sin^2(\theta_W) \right] + \lambda_{1u} \quad (33)$$

$$C_{1d} = \rho' \left[\frac{1}{2} - \frac{2}{3}\kappa' \sin^2(\theta_W) \right] + \lambda_{1d} \quad (34)$$

$$C_{2u} = \rho \left[-\frac{1}{2} + 2\kappa \sin^2(\theta_W) \right] + \lambda_{2u} \quad (35)$$

$$C_{2d} = \rho \left[\frac{1}{2} - 2\kappa \sin^2(\theta_W) \right] + \lambda_{1d} \quad (36)$$

The electroweak radiative correction is well determined in the Standard Model, though other Higgs scenarios and/or new physics at the TeV scale will affect the electroweak correction, offering the opportunity for new physics. Standard Model electroweak radiative corrections to $C_{1,2u(d)}$ have been calculated [54] and are relatively small. The corrections modify the ρ , κ , and λ parameters from their tree level values $\rho = \rho' = \kappa = \kappa' = 1$ and $\lambda_{1u} = \lambda_{1d} = \lambda_{2u} = \lambda_{2d} = 0$. A recent evaluation [55] gives $\rho' = 0.9876$, $\kappa' = 1.0026$, $\rho = 1.0006$, $\kappa = 1.0299$, $\lambda_{1d} = -2\lambda_{1u} = 3.6 \times 10^{-5}$, $\lambda_{2u} = -0.0121$, $\lambda_{2d} = 0.0026$, changing the asymmetry by 2-3% at the Q^2 of the proposed measurement. The error in the SM prediction is dominated by our knowledge of the α , M_Z , M_W , the Higgs mass (very weakly), and $\sin^2 \theta_W$ at the proposed energies. The last is in turn dominated by the Z-pole value: $\sin^2 \theta_W(\text{on shell}) = 0.22306 \pm 0.00033$ from the global fit [55]. Overall, the uncertainty on the EW radiative corrected asymmetry is negligible.

Calculations for PVDIS Radiative Corrections

Methods for radiative corrections for PVDIS were first developed in the late 1980's [56, 57] when results from SLAC E122 were published. In these references, radiative corrections (including both EM and EW) were calculated for the PVDIS asymmetry A_d at the E122 kinematics and for the PVDIS asymmetries A^\pm and the charge (or beam conjugation) asymmetry B for muon scattering experiments at CERN. Should the proposed measurement be approved, we will work closely with theorists to perform a full radiative correction [40].

3.11. Summary of Experimental Systematic Uncertainties

Given the relatively large asymmetry of this measurement, small statistical uncertainty can be achieved with a relatively modest beam allocation. Care must be taken to control the experimental systematic uncertainties at the same level. Expectations for experimental uncertainties are summarized in Tab. IV.

TABLE IV: This table lists the expected systematic uncertainties in the measurement of A_d . These contributions to the uncertainty if the measured asymmetry is to be interpreted in terms of $\sin^2 \theta_W$ are also shown.

Source	$\frac{\delta A_d}{A_d}$	$\frac{\delta \sin^2 \theta_W}{\sin^2 \theta_W}$
Polarization measurement	5.0×10^{-3}	2.5×10^{-3}
Determination of Q^2	3.9×10^{-3}	2.0×10^{-3}
Target Endcaps	1×10^{-3}	0.5×10^{-3}
Target Purity	0.4×10^{-3}	0.22×10^{-3}
Rescatter background	0.2×10^{-3}	0.11×10^{-3}
π^- contamination	0.01×10^{-3}	0.006×10^{-3}
Radiative Corrections	4×10^{-3}	2×10^{-3}
Total	7.6×10^{-3}	3.8×10^{-3}

4. HADRONIC PHYSICS ISSUES

While the experimental challenges described in the previous section are significant, a measurement of A_d approaching $\pm 0.5\%$ (stat) $\pm 0.5\%$ (syst) appears to be feasible. However, there are open questions in hadronic physics at this level of precision which complicate the interpretation of this asymmetry in terms of Standard Model parameters. This section will describe some of these interesting issues.

4.1. Uncertainty from Parton Distributions

As described in Section 2.1, A_d is specified by Standard Model parameters and the parton distribution functions (PDF), with the latter entering Eq. (13) through the ratios R_s and R_v defined in Eqs. (15-16). These PDFs are well described by global fits to world data and additionally some sources of uncertainty (such as Q^2 evolution) may cancel out in these ratios.

The parton distributions provided by CTEQ [58, 59] and MRST [60, 61] also provide uncertainty estimates. These set the scale for the impact of the statistical uncertainties of the global fit on interpretation of A_d at around 0.1%. Both give similar results for the uncertainty in extracting $\sin^2 \theta_W$ from A_d . In particular, CTEQ's parametrization yields $\delta \sin^2 \theta_W / \sin^2 \theta_W = 0.47 \times 10^{-3}$. In addition, the difference between the CTEQ and MRST parton distributions falls well within this uncertainty.

4.2. Uncertainty in R_{LT}

The ratio $R_{LT} = \sigma_L / \sigma_T$ is taken from a global fit, R1998 [62]. It enters A_d through the calculation of the kinematic quantity Y defined in Eq. (14). Propagation of the uncertainty from this fit yields an uncertainty in the extracted value for $\sin^2 \theta_W$ of $\delta \sin^2 \theta_W / \sin^2 \theta_W = 0.08 \times 10^{-3}$.

4.3. Higher-Twist Effects

Among all hadronic effects that could contribute to PV electron scattering observables, the higher-twist (HT) effect is commonly expected to be the most probable for kinematics at Jefferson Lab. Here higher-twist effects refer to the fact that the color interactions between the quarks become observable at low Q^2 and the process cannot be described by the leading twist process of $\gamma(Z)$ exchange between the electron and a single quark. For electro-magnetic scattering processes, these interactions introduce a scaling violation to the structure functions in the low Q^2 region below $1 \text{ GeV}/c^2$ that is stronger than the $\ln(Q^2)$ -dependence described by the DGLAP equations of pQCD. For PV $\vec{e}-^2\text{H}$ scattering, HT effects start from twist-four terms which diminish as $1/Q^2$.

The theory for HT effects is not well established. Most of the knowledge for HT is from experimental data, which itself faces difficult theoretical issues in interpretation. For example, when determining the HT effects from DIS structure functions F_1 and F_2 , the leading twist contribution often cannot be subtracted cleanly because of the uncertainty due to the cutoff in summing the α_s series, and the uncertainty in α_s itself in the low Q^2 region. In another example, the first parametrization of the HT coefficient C_{HT} , performed using a Next-Leading-Order (NLO) pQCD calculation to describe Q^2 evolutions, showed a sizable effect for all x values that increases dramatically at higher x [63]. The latest fit to the HT coefficient, however, shows that the effect for $0.1 < x < 0.4$ diminishes quickly to $< 1\%/Q^2$ as higher order terms (NNLO and NNNLO) are included when evaluating the leading-twist term [61].

By contrast, the prospects for observing HT contributions in PV-DIS are relatively uncomplicated. Many QCD complications which are present in cross-section measurements are suppressed in the parity-violating asymmetry. The observation of any Q^2 -dependent deviation from the expected asymmetry would strongly imply a contribution from HT. With the prospect of pushing precision to the sub-1% level, it may be that parity-violating electron scattering will provide the most accessible method for a transparent study of HT.

Despite the existence of this experimental opportunity, there is almost no information from data on how HT effects PV observables. The 6 GeV PV-DIS experiment E05-007 [13] will be the first one exploring this effect, at moderate x and at two Q^2 value of 1.1 and 1.9 (GeV²). Theoretically, estimates of the twist-four corrections to the asymmetry in $\vec{e}^-^2\text{H}$ scattering have been carried out in various models, with results that do not definitively limit the possible contributions of HT in this kinematic range to negligible levels. In a work by Castorina and Mulders [64], the expansion of the product of electromagnetic and weak currents within the MIT bag model was used to estimate a 0.3% correction to the asymmetry at $Q^2 = 1.0 \text{ GeV}/c^2$ (thus 0.1% to our proposed kinematics). In a similar work by Fajfer and Oakes, an upper limit on the effect was found corresponding to an effect on the asymmetry of $< 1\%$ [65].

Another approach to estimate HT correction to DIS-parity is based on experimental data on C_{HT} and the assumption that the HT effects partly cancel in the numerator and the denominator of the asymmetry. One possible effect that does not cancel comes from the

different coupling strength of the EM and weak interactions in the interference term, which is proportional to the EM and weak charges, respectively. Quantitative calculations for the HT correction to A_d were performed in the QCD LO, NLO and NNLO framework [66], showing the HT correction to A_d is at level of $1\%/Q^2$ for $0.1 < x < 0.3$ in NLO or higher order analysis.

We are in contact with theorists working on a modern estimation of HT effects in PV-DIS from QCD [67]. While this is a challenging topic to address theoretically, we expect to results in about one year.

One interesting remark is that, although the NuTeV measurement was performed at $\langle Q^2 \rangle = 20 \text{ GeV}/c^2$, it can be shown that the HT contribution to the typically measured Paschos-Wolfenstein (P-W) ratio could be of the same magnitude as that to the DIS-parity observable at $Q^2 \approx 2 \text{ GeV}/c^2$ [68]. If the NuTeV deviation from the Standard Model were fully due to higher twist, then this would imply a 1.7% contribution to our proposed measurement. While such a HT contribution is theoretically disfavored for both NuTeV or this proposal, it cannot be strictly ruled out.

It is clear that the HT effects present a significant challenge to the interpretation of this proposed measurement in terms of impact on Standard Model. Most likely, HT effects will only be constrained with the addition of new data. A fully-approved 6 GeV PV-DIS experiment (summarized in App. A) would be an excellent start, providing a first window to glimpse possible HT effects at low Q^2 and moderate x . A more comprehensive study would be enabled by a large acceptance spectrometer, which would extend precision coverage into the high x kinematics where DIS scattering rates are low (see section 6).

4.4. Charge Symmetry Violation (CSV)

Charge symmetry implies the equivalence between the $u(d)$ distributions in the proton and the $d(u)$ distributions in the neutron. This symmetry is trivially violated by the differences in mass and charge between the u and d quarks, but most low energy tests appear to justify the common assumption that this symmetry is good to at least the 1% level on reaction amplitudes [69]. Calculations applying the MIT bag model [70],[71] or the Meson Cloud models [72] have produced results for parton-level CSV ranging from $< 0.1\%$ to a

few percent. Recent global fits of the quark distributions have now also included CSV in valence and sea quarks, either applying theoretical QED corrections in the fit procedure [73] or by introducing a charge-symmetry-violating parameter which could account for both QED splitting and quark mass effects [61]. The subject is particularly germane to precision new-physics searches; CSV effects have become a leading suspected cause for the 3σ deviation from the Standard Model observed by the NuTeV collaboration [74].

The CSV distributions are defined as

$$\delta u(x) = u^p(x) - d^n(x) \quad (37)$$

$$\delta d(x) = d^p(x) - u^n(x) \quad (38)$$

To a good approximation, these CSV parameters enter the expression for the parity-violating asymmetry as a ratio:

$$\frac{\Delta A_d}{A_d} \sim R_{CSV} = 0.3 \frac{\delta u - \delta d}{u + d} \quad (39)$$

Figure 8 shows predicted CSV in parton distribution functions from a theoretical bag model calculation [70] and from purely QED corrections [75]. These predictions represent independent effects and combine contributions in R_{CSV} . While δu and δd are not large compared to the parton distribution functions at low x , at high x these distributions fall more slowly than u and d , leading to an enhancement in R_{CSV} .

For illustrative purposes, one can compare the implied effect on A_d for a calculation using the MIT Bag Model and including QED splitting [75] with that for the MRST QED corrections [73]. Figure 9 shows these effects, plotted against Bjorken x . This suggests that QED splitting alone would provide CSV contributions to A_d at the level of the experimental uncertainty for the proposed measurement, while these contributions may be greatly enhanced by QCD contributions at larger x .

In a separate study, the MRST collaboration included a charge symmetry violating parameter in global PDF fits in an exploration of theoretical (parameterization) uncertainties. This CSV term would account for the QED splitting corrections (which were no longer applied) but also hadronic terms. The particular parameterization chosen for δu and δd falls off rapidly with increasing x ; it should be noted that there is no evidence for or against this assumed behavior, although the fall off is significantly faster than that suggested by calcu-

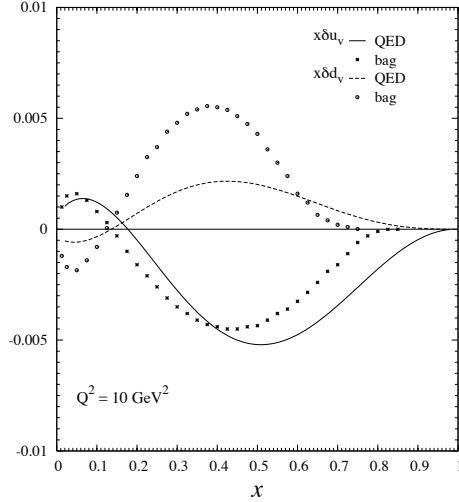


FIG. 8: Charge symmetry violating terms in valence parton distributions from QED splitting alone (solid, dashed) or from QCD effects (circle, square) calculated with a Bag Model. Each of these 4 curves will contribute, additively and with the same sign, to the numerator of R_{CSV} 39.

lations such as those shown in Figure 8. The results are summarized in terms of R_{CSV} in Figure 10. While the central value is consistent with the QED splitting corrections alone, the preference is very weak and the fit allows contributions 4 times larger, or 3 times larger with the opposite sign, within the 90% confidence interval.

These uncertainties reflect the generally poor state of the world experimental data on CSV; the parameters are simply not tightly constrained by existing data. While future experiments may be able to provide significant new constraints on parton level CSV, the effects will be small and challenging to access [76]. (The exception would be precision measurements of PV-DIS at high x , where contributions might easily be a few percent.) A thorough study of the CSV may only be possible with a large acceptance spectrometer described in section 6, which could measure the CSV at a much higher x where the CSV is expected to be prominent, thus constrain the CSV contribution in the x region of the proposed measurement.

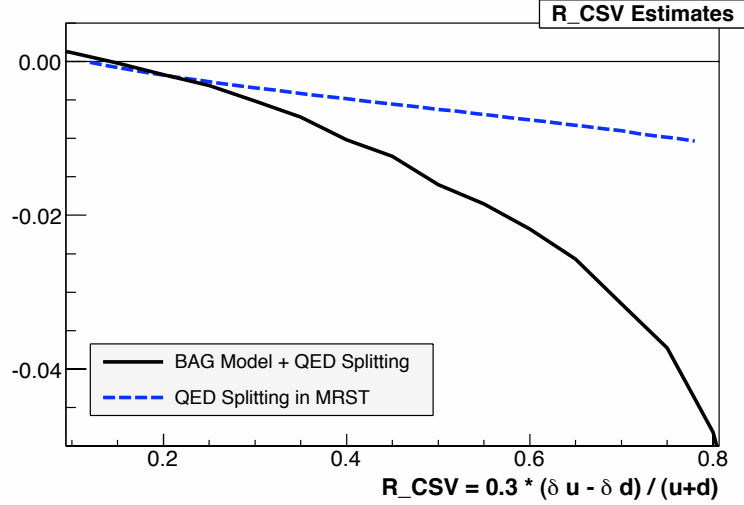


FIG. 9: Predictions for the fractional change in the parity-violating asymmetry $\Delta A_d/A_d$, plotted against x , for the proposed measurement. The MRST prediction [73] includes only QED splitting effects, while the Bag Model + QED splitting prediction [75] includes effects from both quark mass and charge differences.

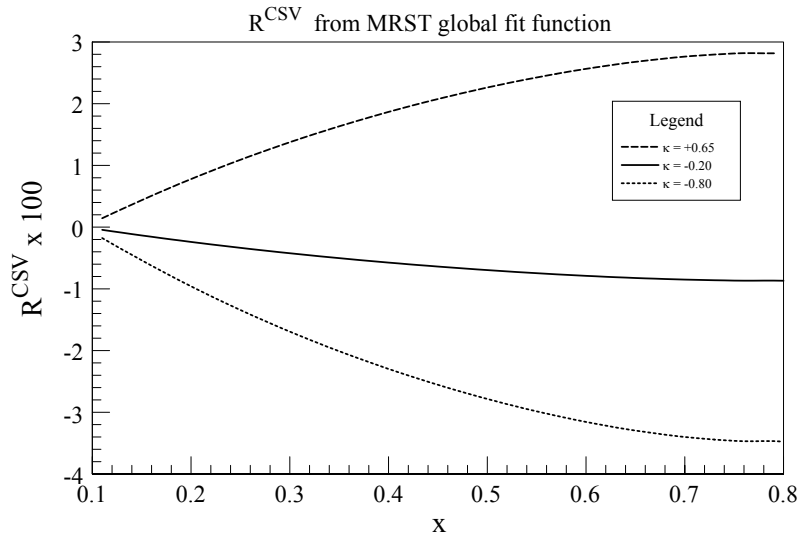


FIG. 10: Fractional change in A_d due to CSV in the MRST global fit [61]. The central value of the fit (CSV parameter $\kappa = -0.2$) suggests effects comparable to the proposed experimental uncertainties, but the 90% allowed region ($-0.8 < \kappa < +0.65$) contains contributions 3-4 times larger.

4.5. Hadronic Uncertainty Summary

While the best estimates from global PDF fits and fits of the R_{LT} ratio suggest uncertainties which are small on the scale of these measurements, there remain significant uncertainties in nucleon partonic structure which will limit the interpretability of results of this proposal in terms of the Standard Model. Higher twist contributions to A_d as large as 0.5% are unlikely, but they can not be ruled out within the limits of existing data or theoretical understanding. The picture of charge symmetry violation is less encouraging, with theoretical understandings pointing to effects at the level of $< 0.5 - 1\%$ but with weak constraints on potentially larger contributions.

While an individual measurement of the asymmetry cannot completely disentangle effects due to partonic CSV, higher twist, or fundamental couplings at odds with the Standard Model values, these effects do have different kinematic dependencies. The well-known signature for HT effects is a contribution which scales as $(1/Q^2)^n$ ($n \geq 1$), whereas CSV should exhibit a weak Q^2 dependence. Both HT and CSV are expected to grow large at high x . The Standard Model parameters $C_{1u(d)}$ and $C_{2u(d)}$ are independent of kinematics, but contribute proportionally according to the kinematic parameter Y [defined in Eq. (14)]. Measurements over a range of x and Q^2 would provide an opportunity to set tight upper limits on contributions from each of these effects independently. With segmentation of kinematics in the fast-counting DAQ, one could provide a small lever arm to examine the changing asymmetry over Q^2 , x , or Y , but a definitive answer would require a more extensive program of measurements.

5. BEAM TIME REQUEST

The goal of this experiment is to achieve 0.5% statistical precision, with comparable systematic uncertainty, on the parity violating asymmetry in deep inelastic scattering, A_d . Because of the relative large asymmetry, $A_d \approx 280$ ppm, this can be realized in a relatively short period of production running – 28 days. Additional beam time will also be needed to study rate effects, particle identification efficiencies, pair production and rescattering backgrounds. These studies were discussed in details in section 3. In addition, we also request for 0.5 day of beam time for optics calibration using a thin carbon (foil) target and 2 days for Moller measurements and invasive studies of the Compton polarimeter. Anticipated beam time requirements for these studies are outlined in Tab. V. Including the various times to study systematic effects, this measurement will require 36 days of beam allocation.

TABLE V: This table outlines the expected beam request and running conditions for production data collection as well as for studies of systematic effects.

Beam Use	Time (days)	E_{beam} (GeV)	I_{beam} (μA)	Target	Spectrometer	HMS, SHMS
					central angle	central momentum (GeV/c)
Production	28	11	85	LD ₂	13.5°	6.0, 5.8
DAQ commissioning and low rate study for Q^2 and PID	2	11	2	LD ₂	13.5°	6.0, 5.8
DAQ deadtime and pileup study (high rate running)	1	11	2-85	LD ₂	13.5°	6.0, 5.8
e^+e^- pair background	0.5	11	85	LD ₂	13.5°	6.0, 5.8
Empty Target Asymmetry	0.6	11	85	Al dummy	13.5°	6.0, 5.8
Optics calibration	0.5	6.6	2	thin ¹² C	13.5°	6.0, 5.8
Elastic measurement for rescattering background	1	6.6	10+	LH ₂	13.5°	4.0-7.0, 3.4-7.5
Invasive Polarimetry Studies	2	11	85	(any)	13.5°	6.0, 5.8
Total	36					

6. COMPLEMENTARITY WITH POSSIBLE LARGE ACCEPTANCE DEVICE PROGRAM

As described in Sec. 4, PV-DIS is sensitive to a combination of the poorly-measured Standard Model parameters $2C_{2u} - C_{2d}$, but also to two open issues in hadronic physics which are interesting in their own right: charge symmetry violation and higher twist. Measurement of A_d over a wide range of Q^2 and x should allow independent constraints on each of these effects. However, low DIS rates make covering a sufficient kinematic range with high precision a significant challenge.

The measurement proposed in this document, while it cannot independently separate these effects, would be probing unexplored territory. Any observed deviation from the expected A_d would be certain to inspire and inform further studies of these interesting hadronic issues and to focus interest on the poorly-measured $C_{2u(d)}$ Standard Model parameters. As an important exploration of poorly-constrained corners of both the Standard Model and QCD, we believe this proposal stands on its own. However, it is our opinion that the value of the present proposal could be enhanced by a broader PV-DIS program using a large acceptance device (in combination with high luminosity).

The effort to develop such a device is underway. Preliminary studies of concepts for this large acceptance device (LAD) suggest that the LAD may be able to cover a suitably large range of x and Q^2 . However, it is very early in the development process, and only first estimates have been made for resolutions, control of backgrounds, and calibration procedures. The proposed measurement covers an area of phase space (low scattering angle, high E') which the LAD concept cannot reach. While the LAD concept nominally covers a range of x and Q^2 which includes the kinematics of the present proposal, the differing angle and E' coverage make this proposal a valuable complement to a LAD program. It may also be that experimental challenges in approaching the ultimately desired systematic precision near 0.5% are best met by a reduced aperture spectrometer such as the HMS/SHMS. These spectrometers have a clear advantage (over the open geometry of a LAD) in determination of the central kinematics, averaging over the accepted kinematics, and in background suppression. If a successful concept is found, the LAD would be able to constrain CSV and HT in kinematic regions where they are expected to be more easily accessible (i.e. high x).

These constraints could then allow a clean interpretation of a high-precision HMS/SHMS point at moderate x in terms of the Standard Model C_{2q} .

It is worth noting that this proposal is optimized for precision in the kinematics best suited to testing the Standard Model, at the ideal point for a high-precision result to complement the LAD program. Given the expected experimental complexity of such a precise measurement, an independent measurement would be a powerful cross-check for establishing the credibility of the result. In our view, this proposed measurement would provide a solid cornerstone for a broader PV-DIS program.

7. CONCLUSION

Parity violation in deep inelastic scattering (PVDIS) has and will continue to play an important role in our understanding of the Standard Model. PVDIS offers sensitivity to the vector Z-electron times axial Z-quark couplings, C_{2q} , not offered by other experiments and thereby provides complementary constraints on processes and particles not included in the Standard Model. At the same time, the asymmetry is relative large, allowing for statistically sensitive measurements to be completed with modest beam time.

The interpretation of this asymmetry in terms of fundamental couplings is potentially clouded by contributions from higher twist and charge symmetry violation. These effects, which are themselves topics of great interest in hadronic physics, can be constrained by further PV-DIS studies over a broad range of x and Q^2 . Such a program is not feasible with existing spectrometers at Jefferson Lab, but will likely motivate the development of a new, dedicated large acceptance apparatus. Such a device could be used to study these hadronic effects at kinematics where they are prominent. The proposed measurement, with very high systematic accuracy, statistical precision, and kinematics optimized for sensitivity to the C_{2q} couplings, would have its value enhanced by the constraints provided by such a program. PV-DIS with the HMS/SHMS would serve as a crucial cornerstone to a broader program of PVDIS study with a large acceptance apparatus.

We propose a measurement of parity violation asymmetry in \vec{e}^- - ^2H DIS at $Q^2 = 3.3 \text{ GeV}^2$, $\langle W^2 \rangle = 7.3 \text{ GeV}^2$ and $\langle x \rangle = 0.34$. With a total beam allocation of 36 days, an uncertainty on the asymmetry of $\delta A_d/A_d = \pm 0.005(\text{stat.}) \pm 0.006(\text{syst.})$ can be achieved. Assuming hadronic

effects are small, the weak coupling constant combinations $2C_{2u} - C_{2d}$ and the value of $\sin^2 \theta_W$ could be extracted with uncertainties of $\delta(2C_{2u} - C_{2d}) = \pm 0.015(stat.) \pm 0.018(exp.syst.)$ and $\delta \sin^2 \theta_W / \sin^2 \theta_W = \pm 0.0025(stat.) \pm 0.0032(expt.syst.)$. These results could provide constraints on different possible extensions of the Standard Model. Or, one can extract from A_d constraints on hadronic effects such as higher twists and charge symmetry violations if assuming the Standard Model is exact. Approval of this proposal would no doubt open a new era in DIS experiments, in which PV observables are used to study both electroweak and hadronic physics.

APPENDIX A: RELATION TO PV-DIS AT 6 GEV (JLAB E05-007)

Some of the motivation for this 12 GeV experiment is similar to the 6 GeV PV-DIS experiment (JLab E05-007), which is summarized in Tab. VI. Both experiments are using

	I	II
x	0.25	0.30
Q^2 [GeV ²]	1.1	1.9
W^2 [GeV ²]	4.2	5.3
A_D [ppm]	-91	-161
Phase I: $\delta A_D / A_D$ [%]	3.5	6.0
Phase II: $\delta A_D / A_D$ [%]	2.5	2.4

TABLE VI: Summary of kinematics and total experimental precision of planned PV-DIS experiment E05-007 at 6 GeV. Phase I has been approved with an A- rating.

parity violation in deep inelastic scattering, but the goals of these two experiments are quite complementary. The 6 GeV PV-DIS experiment will be studying the Q^2 dependence of A_d , with a possible extraction of the weak couplings $2C_{2u} - C_{2d}$. As such, the 6 GeV PV-DIS measurement is important to the interpretation of the measurement proposed here, since they will constrain the $1/Q^2$ dependence of possible higher twist hadronic effects (see Sec. 4.3). As a probe of the Standard Model, the 6 GeV PV-DIS experiment, while good, lacks the statistical and systematic sensitivity of this proposed measurement. In addition,

the measurement proposed here is at kinematics (both higher Q^2 and W^2) which put it firmly into the DIS region.

APPENDIX B: TECHNICAL PARTICIPATION OF ARGONNE NATIONAL LABORATORY

The Physics Division at Argonne National Laboratory is actively involved in this proposal for JLab Hall C. The Argonne Group is responsible for the initial optics design of the SHMS and for the spectrometer field maps and verification of the SHMS optics. In addition, should this proposal be approved, the Argonne group will make a commitment to the realization of the Compton Polarimeter for Hall C.

APPENDIX C: CONTRIBUTIONS FROM THE UNIVERSITY OF VIRGINIA

Two of the three spokespersons of this proposal are from University of Virginia (UVa), and one of the spokespersons already has a conditionally approved experiment for Hall C using the 11 GeV beam with commitment of 1 FTE-year to the beamline commissioning, including the Compton and the Moller polarimetry, the ARC energy measurement and the raster system. The other spokesperson is committed to significant contributions to the Hall C Compton through participation in the QWeak collaboration. The UVa group will continue this level of commitment to the beamline commissioning and the Compton polarimetry in Hall C at 12 GeV in support of a precision asymmetry measurement program.

-
- [1] M. J. Ramsey-Musolf, Phys. Rev. **C60**, 015501 (1999), hep-ph/9903264.
 - [2] S. Eidelman et al. (Particle Data Group), Phys. Lett. **B592**, 1 (2004).
 - [3] M. S. Chanowitz, Phys. Rev. Lett. **87**, 231802 (2001), hep-ph/0104024.
 - [4] M. S. Chanowitz, Phys. Rev. **D66**, 073002 (2002), hep-ph/0207123.
 - [5] S. C. Bennett and C. E. Wieman, Phys. Rev. Lett. **82**, 2484 (1999), hep-ex/9903022.
 - [6] G. P. Zeller et al. (NuTeV), Phys. Rev. Lett. **88**, 091802 (2002), hep-ex/0110059.
 - [7] P. L. Anthony et al. (SLAC E158), Phys. Rev. Lett. **95**, 081601 (2005), hep-ex/0504049.

- [8] D. Armstrong et al. (2001), JLab E02-020.
- [9] J. Erler and M. J. Ramsey-Musolf, Phys. Rev. **D72**, 073003 (2005), hep-ph/0409169.
- [10] J. Erler and M. J. Ramsey-Musolf, Prog. Part. Nucl. Phys. **54**, 351 (2005), hep-ph/0404291.
- [11] E. J. Beise, M. L. Pitt, and D. T. Spayde, Prog. Part. Nucl. Phys. **54**, 289 (2005), nucl-ex/0412054.
- [12] A. Argento et al., Phys. Lett. **B120**, 245 (1983).
- [13] P. E. Reimer, R. Michaels, X. Zheng, and the Hall A Collaboration (2005), JLab E05-007.
- [14] C. Y. Prescott et al., Phys. Lett. **B77**, 347 (1978).
- [15] C. Y. Prescott et al., Phys. Lett. **B84**, 524 (1979).
- [16] K. A. Aniol et al. (HAPPEX), Phys. Rev. Lett. **96**, 022003 (2006), nucl-ex/0506010.
- [17] D. S. Armstrong et al. (G0), Phys. Rev. Lett. **95**, 092001 (2005), nucl-ex/0506021.
- [18] R. Hasty et al. (SAMPLE), Science **290**, 2117 (2000), nucl-ex/0102001.
- [19] R. N. Cahn and F. J. Gilman, Phys. Rev. **D17**, 1313 (1978).
- [20] R. Arnold et al. (1993), SLAC-PROPOSAL-E-149.
- [21] A. E. Nelson, Phys. Rev. Lett. **78**, 4159 (1997), hep-ph/9703379.
- [22] J. Erler, A. Kurylov, and M. J. Ramsey-Musolf, Phys. Rev. **D68**, 016006 (2003), hep-ph/0302149.
- [23] J. Erler, *priv. comm.*
- [24] D. London and J. L. Rosner, Phys. Rev. **D34**, 1530 (1986).
- [25] P. Langacker, M.-x. Luo, and A. K. Mann, Rev. Mod. Phys. **64**, 87 (1992).
- [26] E. Eichten, K. D. Lane, and M. E. Peskin, Phys. Rev. Lett. **50**, 811 (1983).
- [27] D. Zeppenfeld and K.-M. Cheung (1998), hep-ph/9810277.
- [28] K.-m. Cheung, Phys. Lett. **B517**, 167 (2001), hep-ph/0106251.
- [29] C. Adloff et al. (H1), Z. Phys. **C74**, 191 (1997), hep-ex/9702012.
- [30] J. Breitweg et al. (ZEUS), Z. Phys. **C74**, 207 (1997), hep-ex/9702015.
- [31] E. Leader and E. Predazzi, *An Introduction to Gauge Theories and Modern Particle Physics* (Cambridge University Press, 1996).
- [32] A. Kurylov, M. J. Ramsey-Musolf, and S. Su, Phys. Lett. **B582**, 222 (2004).
- [33] J. Arrington, P. Bosted, H. Mkrтчyan, X. Zheng, and the Hall A Collaboration (2007), JLab PR06-005 and PR07-010.

- [34] J. Arrington et al. (Hall C), *Conceptual design report Hall C 12 gev upgrade* (2002).
- [35] J. Arrington et al., *Pre-conceptual design report (pCDR) for the science and experimental equipment for the 12 GeV upgrade of CEBAF* (2004).
- [36] A. Bruell, P. Brindza, R. Ent, D. Potterveld, and C. Yan, *priv. comm.* (2006).
- [37] D. E. Wiser, Ph.D. thesis, University of Wisconsin (1977), UMI 77-19743.
- [38] A. Airapetian et al. (HERMES), *Phys. Rev. Lett.* **84**, 4047 (2000), hep-ex/9910062.
- [39] H. Avakian et al. (CLAS), *Phys. Rev.* **D69**, 112004 (2004), hep-ex/0301005.
- [40] A. Afanasev, *priv. comm.*
- [41] *Happex-h (e99-115) and happex-he (e00-114) experiments* (2005), URL <http://hallaweb.jlab.org/experiment/HAPPEX/>.
- [42] P. Souder, Z.-E. Meziani, J.-P. Chen, et al. (1999), JLab E99-117.
- [43] R. Michaels, P. Souder, G. Urciuoli, et al. (2006), JLab E06-002.
- [44] M. Hauger et al., *Nucl. Instrum. Meth. A* **462**, 382 (2001), nucl-ex/9910013.
- [45] L. Levchuck, *Nucl. Instrum. Meth.* **A345**, 496 (1994).
- [46] N. Sherman, *Phys. Rev.* **103**, 1601 (1956).
- [47] M. Woods (SLD) (1996), hep-ex/9611005.
- [48] A. Acha et al. (HAPPEX), *Phys. Rev. Lett.* **98**, 032301 (2007), nucl-ex/0609002.
- [49] M. Seely, *Gas chromatograph analysis for deuterium sample* (2002).
- [50] D. Meekins (2007), URL http://www.jlab.org/~meekins/Target_Configs/HallA/April_2007/halla_config_11_27_06.htm.
- [51] M. E. Christy et al. (E94110), *Phys. Rev.* **C70**, 015206 (2004), nucl-ex/0401030.
- [52] L. W. Mo and Y.-S. Tsai, *Rev. Mod. Phys.* **41**, 205 (1969).
- [53] R. Arnold, P. Bosted, and S. Rock (2003), SLAC-LOI-2003-1.
- [54] W. J. Marciano and A. Sirlin, *Phys. Rev. D* **29**, 75 (1984).
- [55] W.-M. Yao, C. Amsler, D. Asner, R. Barnett, J. Beringer, P. Burchat, C. Carone, C. Caso, O. Dahl, G. D'Ambrosio, et al., *Journal of Physics G* **33**, 1+ (2006), URL <http://pdg.lbl.gov>.
- [56] D. Y. Bardin, O. M. Fedorenko, and N. M. Shumeiko, *Sov. J. Nucl. Phys.* **32**, 403 (1980).
- [57] D. Y. Bardin, O. M. Fedorenko, and N. M. Shumeiko, *J. Phys.* **G7**, 1331 (1981).
- [58] D. Stump et al., *Phys. Rev.* **D65**, 014012 (2002), hep-ph/0101051.

- [59] J. Pumplin et al., Phys. Rev. **D65**, 014013 (2002), hep-ph/0101032.
- [60] A. D. Martin, R. G. Roberts, W. J. Stirling, and R. S. Thorne, Eur. Phys. J. **C28**, 455 (2003), hep-ph/0211080.
- [61] A. D. Martin, R. G. Roberts, W. J. Stirling, and R. S. Thorne, Eur. Phys. J. **C35**, 325 (2004), hep-ph/0308087.
- [62] K. Abe et al. (E143), Phys. Lett. **B452**, 194 (1999), hep-ex/9808028.
- [63] M. Virchaux and A. Milsztajn, Phys. Lett. **B274**, 221 (1992).
- [64] P. Castorina and P. J. Mulders, Phys. Rev. **D31**, 2760 (1985).
- [65] S. Fajfer and R. J. Oakes, Phys. Rev. **D30**, 1585 (1984).
- [66] W. van Neerven, *priv. comm.*
- [67] M. Ramsey-Musolf, *priv. comm.*
- [68] M. Gluck and E. Reya, Phys. Rev. Lett. **47**, 1104 (1981).
- [69] G. A. Miller, B. M. K. Nefkens, and I. Slaus, Phys. Rep. **194**, 1 (1990).
- [70] E. N. Rodionov, A. W. Thomas, and J. T. Londergan, Mod. Phys. Lett. **A9**, 1799 (1994).
- [71] J. T. Londergan and A. W. Thomas, Phys. Rev. **D67**, 111901 (2003).
- [72] F.-G. Cao and A. I. Signal, Phys. Rev. **C62**, 015203 (2000).
- [73] A. D. Martin, R. G. Roberts, W. J. Stirling, and R. S. Thorne, Eur. Phys. J. **C39**, 155 (2005), hep-ph/0411040.
- [74] J. T. Londergan and A. W. Thomas (2004), hep-ph/0407247.
- [75] M. Gluck, P. Jimenez-Delgado, and E. Reya, Phys. Rev. Lett. **95**, 022002 (2005), hep-ph/0503103.
- [76] J. T. Londergan, D. P. Murdock, and A. W. Thomas, Phys. Rev. **D72**, 036010 (2005), hep-ph/0507029.